

1 **Systematics and phylogeography of the Mediterranean *Helichrysum pendulum***  
2 **complex (Compositae) inferred from nuclear and chloroplast DNA and**  
3 **morphometric analyses**  
4

5  
6 **Sonia Herrando-Moraira<sup>1</sup>, Pau Carnicero<sup>2</sup>, José M. Blanco-Moreno<sup>3</sup>, Llorenç Sáez<sup>2,4</sup>, Errol Véla<sup>5</sup>,**  
7 **Roser Vilatersana<sup>1</sup> & Mercè Galbany-Casals<sup>2</sup>**  
8

9 1 Institut Botànic de Barcelona (IBB-CSIC-ICUB), 08038 Barcelona, Spain

10 2 Departament de Biologia Animal, Biologia Vegetal i Ecologia, Universitat Autònoma de Barcelona, ES-  
11 08193 Bellaterra, Spain

12 3 Departament de Biologia Evolutiva, Ecologia i Ciències Ambientals & IRBio Universitat de Barcelona,  
13 Av. Diagonal 643, ES-08028 Barcelona, Spain

14 4 Societat d'Història Natural de les Illes Balears (SHNB). C. Margarida Xirgu 16. ES-07003 Palma de  
15 Mallorca, Balearic Islands, Spain

16 5 UMR AMAP, Université Montpellier 2, 34398 Montpellier, France

17  
18 Author for correspondence: Sonia Herrando-Moraira, [sonia.herrando@gmail.com](mailto:sonia.herrando@gmail.com)  
19

20 ORCID: S.H.M, <http://orcid.org/0000-0002-0488-5112>  
21

22 **Abstract** Multiple factors related to complex geomorphological and climatic history, in addition to other  
23 biological factors such as hybridization, hinder the definition of some Mediterranean plant groups. The  
24 existence of controversial taxonomic treatments, the possible hybridization events involved, and its  
25 unknown evolutionary history, make the *Helichrysum pendulum* complex of sect. *Stoechadina* an ideal  
26 model to understand general processes about Mediterranean plant systematics and evolution. The mosaic  
27 range of the complex, which is distributed over several islands and continental areas in the western-  
28 central Mediterranean Basin, provides an opportunity to investigate how past connections and  
29 disconnections between landmasses may have determined the current geographic distribution of genetic  
30 variation in this area. The cpDNA region *rpl32-trnL* intergenic spacer and the nrDNA region ETS were  
31 sequenced for 1–8 individuals from each of the 44 populations sampled, covering all taxa and the whole  
32 geographic range of the complex. These individuals were analysed together with a broad sampling of the  
33 remaining members of sect. *Stoechadina*. In addition, detailed multivariate analyses of morphological  
34 characters were performed for the whole section and for the *H. pendulum* complex. Considering together  
35 distinctive genetic and morphological traits, our species concept is presented and discussed in a context of  
36 integrative taxonomy, and five species are recognized within the complex: *H. errerae*, *H. melitense*, *H.*  
37 *pendulum*, *H. saxatile* and *H. valentinum*. The first three species are recognizable by qualitative and  
38 quantitative morphological traits, and are genetically distinguishable from the rest as shown by the  
39 molecular markers analysed. The two last species are reported here to have a putative ancient hybrid  
40 origin and are also genetically distinguishable from the rest but morphologically recognisable only by  
41 quantitative characters. Phylogenetic relationships shown by nuclear and chloroplast markers, and an  
42 intermediate morphology between the two putative parental taxa, point to *H. pendulum* and *H. italicum* as  
43 the putative parental taxa for *H. saxatile*, and *H. pendulum* and *H. stoechas* as putative parental taxa for  
44 *H. valentinum*. In a discriminant analysis of the five species, 97.8% of all individuals were classified  
45 correctly. The high level of haplotype and ribotype diversity observed in North Africa indicates that this  
46 region is either the area of origin of the complex or a secondary contact zone. Our results suggest that the  
47 complex colonized several islands and migrated through the Gibraltar and Sicilian Straits during phases  
48 of low sea level, favoured by local dispersal events that promoted its gradual range expansion. The  
49 occurrence of the complex in the Balearic Islands, which have remained isolated even during low sea  
50 level phases, could be explained by stochastic long-distance dispersal events.  
51

52 **Keywords** canonical discriminant analysis; ETS; integrative taxonomy; phylogenetic incongruence;  
53 principal component analysis; *rpl32-trnL*.

54  
55 **Supplementary Material** Electronic Supplement (Tables S1, S2; Figs. S1, S2, S3, S4, S5; Appendix  
56 S1, S2) and DNA sequence alignments are available in the Supplementary Data section of the online  
57 version of this article at <http://ingentaconnect.com/content/iapt/tax>  
58

59  
60 **Short title** Systematics of the *Helichrysum pendulum* complex  
61  
62

## 63 ■ INTRODUCTION

64  
65 There is an increasing interest in understanding the complexity of currently observed genetic  
66 patterns and in clarifying the systematics of plant species in the Mediterranean Basin (e.g., [Zozomová-](#)  
67 [Lihová & al., 2014](#)). Gene flow among populations, genetic drift and intrinsic biological traits are  
68 necessary but not sufficient to explain the distribution and diversity of species ([Troia & al., 2012](#)). Two  
69 other factors are decisive for the complex evolution of species: geomorphological history and climate  
70 variation ([Thompson, 2005](#)). The Mediterranean Basin, which is recognized as one of the global  
71 biodiversity hotspots ([Myers & al., 2000](#); [Thompson, 2005](#)), has been heavily influenced by  
72 geomorphological and climatic changes since its formation ([Woodward, 2009](#)). During the Messinian  
73 Salinity Crisis (MSC) (5.96–5.33 Ma; [Hsü & al., 1977](#)), the Strait of Gibraltar closed and the  
74 Mediterranean sea level dropped because of intense evaporation. Subsequently, a desert area emerged,  
75 allowing the establishing of land bridges between southern Europe and northern Africa ([Duggen & al.,](#)  
76 [2003](#)) and between some currently isolated areas in the Mediterranean Basin ([Beerli & al., 1996](#)). This  
77 area promoted the migration and colonization of new areas by organisms that would otherwise have  
78 remained within narrower geographical areas because of reduced dispersal ability. The subsequent  
79 refilling of the Mediterranean Basin following the reopening of the Gibraltar Strait (5.3 Ma, beginning of  
80 the Pliocene) resulted in the geographical fragmentation of the distribution areas of those organisms  
81 which expanded across the Mediterranean Basin ([Beerli & al., 1996](#)). Afterwards, during the Pleistocene  
82 glacial periods, the sea level again dropped, and some of the Mediterranean islands reconnected between  
83 them or to the mainland, allowing gene flow between populations, e.g., Sicily with other islands in this  
84 region such as Malta, and the Aegadian Archipelago ([Fernández-Mazuecos & Vargas, 2011](#); [Lo Presti &](#)  
85 [Oberprieler, 2011](#)). These recurrent connections and disconnections of landmasses in Europe and Africa  
86 have been considered important modulators of the phylogeography across the region ([Nieto-Feliner,](#)  
87 [2014](#)). One of the modulators are straits such as the Strait of Gibraltar and the Sicilian Channel, which  
88 have played alternative roles as a bridge or a barrier to dispersal, allowing migration and diversification  
89 processes, respectively ([Lavergne & al., 2013](#)). While for many plant species straits have caused  
90 significant genetic differentiation ([Fiz & al., 2002](#); [Rubio de Casas & al., 2006](#); [Terrab & al., 2008](#)),  
91 different studies have also documented gene flow between populations on both sides of straits ([Ortiz &](#)  
92 [al., 2007](#); [Guzmán & Vargas, 2009](#); [Fernández-Mazuecos & Vargas, 2011](#); [Lo Presti & Oberprieler, 2011](#)).

93 The complex taxonomic problems found in some Mediterranean plant groups are hypothesised to  
94 be due to the effects of the environmental factors named above, related to geomorphological and climatic  
95 history, but also to biological factors such as hybridization (e.g., [Koch & al., 2016](#)). In recent decades,  
96 taxonomy has undergone a renaissance with the application of DNA methods in addition to the traditional  
97 morphology-based comparisons. The combination of multidisciplinary data for species delimitation has  
98 been termed “integrative taxonomy” ([Dayrat, 2005](#); [Schlick-Steiner & al., 2010](#)). Species limits proposed  
99 by morphological taxonomy (iterative taxonomy; [Yeates & al., 2010](#)) may be verified by independent  
100 information provided from multiple and complementary perspectives, such as phylogeography,  
101 population genetics or ecology. The application of integrative taxonomy has proven useful to resolve  
102 conflicting taxonomic treatments of complex Mediterranean groups of species (e.g., [Koch & al., 2016](#)).

103 The *Helichrysum pendulum* aggr. (Greuter, 2006+) (Gnaphalieae, Compositae) is a complex of  
104 closely related shrubby or sub-shrubby species in sect. *Stoechadina* (DC.) Gren. & Godr. (Galbany-Casals  
105 & al., 2006a). The taxa in the complex are distributed among several islands and continental areas across  
106 the western-central Mediterranean region. They grow within a wide altitudinal range (0–1850 m) and  
107 inhabit diverse habitats such as limestone rock crevices in mountain areas, maritime cliffs or scrubland  
108 formations. Morphological discontinuities found across the fragmented distribution area have led to the  
109 recognition of numerous taxa at specific and infraspecific levels by several authors (Nyman, 1879; Fiori,  
110 1927; Clapham, 1976; Pignatti, 1982). There are numerous alternative taxonomic treatments, and the  
111 most recent ones vary from the recognition of only two (Galbany-Casals & al., 2006a) to nine species  
112 (Greuter, 2006+). Some of the analytical treatments focused on a specific geographical area and therefore  
113 could not capture the complete morphological variation of the complex (e.g., Clapham, 1976; Pignatti,  
114 1982; Scialabba & al., 2008), whereas others were comprehensive (Greuter, 2006+). However, none  
115 provided a detailed analysis of the morphological data, an explanation of the adopted species concept, or  
116 in some cases (Greuter, 2006+; Scialabba & al., 2008) even an identification key.

117 Galbany-Casals & al. (2006a) provided a detailed taxonomic treatment of the entire sect.  
118 *Stoechadina*, in which the *Helichrysum pendulum* complex was reduced to two species that were clearly  
119 distinguishable based on qualitative characters: *Helichrysum errerae* Tineo, which is endemic to  
120 Pantelleria Island, was characterized by herbaceous outermost involucral bracts that are completely or  
121 partially covered with a dense indumentum. *Helichrysum pendulum* (C. Presl) C. Presl (as *H. rupestre*  
122 Raf.), a widely distributed species that included most of the taxa previously described in the complex, was  
123 characterized by papery and glabrous outermost involucral bracts. After studying numerous specimens  
124 from the entire range, as well as the types of all involved taxa, these authors concluded that the extensive  
125 morphological variability in several traits within *H. pendulum* did not follow a clear pattern of correlation,  
126 or it presented a high level of overlap among the taxa recognised in other treatments. Overall, these  
127 authors considered that the absence of qualitative characters would not allow the unequivocal  
128 identification of many specimens, preventing the recognition of most previously proposed taxa.

129 However, the study conducted by Galbany-Casals & al. (2006a) had several shortcomings. First, it  
130 did not include a multivariate analysis of morphological variation, and the continuous variation in  
131 quantitative characters received little attention. Second, the number of studied specimens in some taxa  
132 was very limited and only based on herbarium specimens (e.g., *Helichrysum melitense* (Pignatti) Brullo,  
133 Lanf., Pavone & Ronsiv.). Additionally, the study did not include molecular data. Finally, although  
134 morphologically intermediate specimens between several pairs of species were documented—some of  
135 them were derived from current hybridization and others apparently from an ancient hybridization—it  
136 was not clearly stated whether, and in which cases, specimens originating from hybridization should be  
137 considered to constitute species.

138 The last point is crucial, given that the impact of hybridization on the evolution of *Helichrysum*  
139 Mill. has recently been highlighted (Galbany-Casals & al., 2012, 2014). On the one hand, hybridization  
140 followed by backcrossing with parental taxa is currently occurring between clearly different species. This  
141 phenomenon has been identified in the field by the occurrence of occasional morphologically  
142 intermediate specimens that grow in the vicinity of both putative parental species (Galbany-Casals & al.,  
143 2006a, 2012; and M. Galbany-Casals and L. Sáez pers. obs. in Mallorca, Sardinia, Ibiza, Crete and  
144 Rhodes). In particular, current hybridization events between two species of different sections and  
145 backcrossing of hybrids with parental taxa have been demonstrated in a combined study that included  
146 multivariate analyses of morphological traits and molecular data (Galbany-Casals & al., 2012).

147 On the other hand, historical or past hybridization events probably also occurred repeatedly, as  
148 evidenced by molecular studies of the genus focused on phylogeny and biogeography (Galbany-Casals &  
149 al., 2009, 2014). Past hybridization events can sometimes have been the origin of entire lineages, as  
150 observed for the entire Mediterranean-Macaronesian-Asiatic clade of *Helichrysum*, which has been  
151 postulated to have originated by allopolyploidy (Smitsen & al., 2011; Galbany-Casals & al., 2014).  
152 Additionally, past hybridization events have been proposed to explain the origin of certain taxa. In  
153 particular, *H. valentinum* Rouy, a member of the *H. pendulum* complex from the eastern Iberian  
154 Peninsula, has been suggested to have an ancient hybrid origin between *H. pendulum* and *H. stoechas* (L.)  
155 Moench (Galbany-Casals & al., 2006a). This hypothesis was based on the morphologically intermediate

156 status between these two species although *H. pendulum* currently does not grow in the distribution area of  
157 *H. valentinum*. However, *H. valentinum* grows together with *H. stoechas*, with which it probably also  
158 hybridizes (M. Galbany-Casals, pers. obs.). The complexity of this case has not been satisfactorily  
159 resolved. To date, contemporary or historical hybridization within the *H. pendulum* complex or with other  
160 taxa of sect. *Stoechadina* has not been explored using molecular and morphometric data.

161 For this study, we performed extensive sampling of the whole *Helichrysum pendulum* complex.  
162 We used detailed multivariate morphometric analyses and two molecular markers: the cpDNA *rpl32-trnL*  
163 intergenic spacer and the nrDNA external transcribed spacer (ETS). These markers were chosen for two  
164 main reasons: (1) they often contain enough variation within and among plant species populations and  
165 consequently are useful in low taxonomic level analyses (Baldwin & Markos, 1998; Shaw & al., 2007);  
166 (2) they are available for many species of *Helichrysum* (Galbany-Casals & al., 2009, 2014). Furthermore,  
167 cpDNA has been widely used in plant phylogenetics and phylogeography given its non-recombinant  
168 nature. Given that cpDNA is usually maternally inherited (Corriveau & Coleman, 1988), it can be used to  
169 infer colonization patterns by seeds (Lee & al., 2013). In addition, the ETS region permits the deduction  
170 of gene flow by seeds and pollen because it is biparentally inherited and, in comparison to other nrDNA  
171 regions and to cpDNA, highly variable, so that it can be used in studies of young lineages (Lee & al.,  
172 2013). Moreover, the presence of multiple copies of nrDNA in the genome can reflect recent gene flow or  
173 hybridization events through the coexistence of parental copies (Grimm & Denk, 2008).

174 The aims of this paper are as follows: (1) to unravel genetic variation and phylogeographic  
175 patterns in the *H. pendulum* complex, using molecular data and phylogenetic analyses of the *H. pendulum*  
176 complex in the context of the whole of sect. *Stoechadina*, and analyses of the geographic structure and  
177 molecular variance of the *H. pendulum* complex; (2) to clarify the systematics of the *H. pendulum*  
178 complex and provide a consistent taxonomic treatment based on genetic and morphological data, using  
179 multivariate analyses of morphological data, which will be performed following several successive steps.  
180 Initially, Principal Component Analyses (PCA) will serve to assess the distribution of all morphological  
181 variation in the entire sect. *Stoechadina*, particularly in the *H. pendulum* complex. The results, combined  
182 with genetic data—e.g., exclusive ribotypes or haplotypes, and the relationships between them—will be  
183 interpreted to propose a taxonomic treatment. Finally, this proposal will be further discussed and tested  
184 using additional PCA and Canonical Discriminant Analysis (CDA) of morphological data.

## 185 186 187 ■ MATERIALS AND METHODS

188  
189 **Sampling strategy.** — We collected 44 populations belonging to all taxa described within the *H.*  
190 *pendulum* complex (as delimited in Greuter, 2006+) and covering their entire distribution ranges (see  
191 Figs. 1B, 2A; Electr. Suppl.: Table S1). To take into account all possible existing taxa in the complex, we  
192 initially considered 11 putative different taxa based on the most recent and analytical classifications  
193 (Greuter, 2006+; Scialabba & al., 2008; Mateo & al., 2013; Xiberras, 2013). With the aim of  
194 characterizing the genetic structure and variation across the group, population sampling on a region-wide  
195 scale was favoured over within-population sampling, and thus one to eight individuals per population  
196 were sampled. *Helichrysum stoechas* is morphologically very similar to some members of the complex. It  
197 does not differ in terms of qualitative characters, and *H. stoechas* and the *H. pendulum* complex can  
198 partially overlap in their range of variation of most quantitative characters. However, *H. stoechas* has not  
199 been considered a member of this complex in any recent treatment or flora, undoubtedly because of its  
200 less robust habit and different ecological preferences, making it readily distinguishable in the field.  
201 Confusion between *H. stoechas* and taxa of the *H. pendulum* complex can only be caused by particular  
202 herbarium specimens. *Helichrysum pomelianum* Greuter was deliberately excluded from this study  
203 because it was considered to be part of the morphological variation of *H. stoechas* in Galbany-Casals &  
204 al. (2006b). In addition, 57 specimens belonging to 30 different taxa (26 *Helichrysum* species, five  
205 subspecies and *Anaphalis margaritacea* (L.) Benth. & Hook.f.) were included in some analyses to test the  
206 phylogenetic relationships and to identify possible hybridization events between members of the *H.*  
207 *pendulum* complex and other species of *Helichrysum* (see Electr. Suppl.: Table S1). This sampling

208 focused on other species of the Mediterranean-Macaronesian-Asiatic clade and, in particular, on members  
209 of sect. *Stoechadina* based on previous studies examining morphology, phylogeny and hybridization  
210 (Galbany-Casals & al., 2006a, 2009, 2012, 2014).

211 In the morphological analysis, which included several analyses with different aims (see below), we  
212 sampled 380 individuals of all taxa of sect. *Stoechadina*, of which 136 belonged to the *H. pendulum*  
213 complex (see [Electr. Suppl.: Appendix S1](#) for the list of all specimens examined). Given that the main  
214 aims of the paper were to unravel the evolutionary history and phylogeographic patterns of the *H.*  
215 *pendulum* complex, and to infer the putative ancient hybrid origin of some of the taxa, but not to explore  
216 the existence of ongoing hybridization between species of the *H. pendulum* group and other species of  
217 sect. *Stoechadina*, occasional morphologically intermediate specimens were not included here. The study  
218 of current hybridization would require specific attention in a separate work.

219  
220 **DNA extraction, amplification and sequencing.** — Leaf material was collected in the field  
221 and immediately dried in silica gel. Total genomic DNA was extracted following the CTAB method of  
222 [Doyle & Dickson \(1987\)](#) as modified by [Cullings \(1992\)](#) and [Tel-Zur & al. \(1999\)](#). The quantity of each  
223 DNA extraction was checked using NanoDrop-1000 (Thermo Scientific, Wilmington, DE, USA), and the  
224 quality was evaluated on a 1.2% agarose gel.

225 Amplification and sequencing of the ETS region was performed using the forward primer ETS1f  
226 ([Linder & al., 2000](#)) and the reverse primer 18S-ETS ([Markos & Baldwin, 2001](#)); for *rpl32-trnL*, the  
227 forward primer rpl32F and the reverse primer trnL<sup>(UAG)</sup> ([Shaw & al., 2007](#)) were used. Polymerase chain  
228 reaction (PCR) amplifications were conducted using the reaction mixture described by [Barres & al.](#)  
229 ([2011](#)). The profiles used for amplification were as described by [Galbany-Casals & al. \(2009, 2010\)](#).  
230 Nucleotide sequencing was performed at “Parque Científico de Madrid” on an ABI 3730 DNA analyser  
231 (Applied Biosystems, Foster City, California, USA) or at the DNA Sequencing Core, CGRC/ICBR of the  
232 University of Florida on an ABI 3730xl DNA analyser (Applied Biosystems). In total, 253 *rpl32-trnL*  
233 sequences and 202 ETS sequences were included in this study, of which 229 and 175, respectively, were  
234 new (see [Electr. Suppl.: Appendix S2](#) for accession numbers).

235  
236 **Network representation and phylogenetic analyses.** — The sequences were edited and  
237 aligned by hand using Chromas v.2.0 (Technelysium, Tewantin, Australia) and MEGA v.6 ([Tamura & al.,](#)  
238 [2013](#)). Data matrices are available in the Supplementary Data section of the online version of this article  
239 at <http://ingentaconnect.com/content/iapt/tax>.

240 The *rpl32-trnL* and the ETS datasets included, respectively, 216 and 159 specimens belonging to  
241 the *H. pendulum* complex. Regions that were rich in poly-T and poly-A were manually excluded, as well  
242 as other regions with an ambiguous alignment. In the case of ETS, as previously reported by [Conesa & al.](#)  
243 ([2012](#)), we found several sequenced specimens with intraindividual polymorphisms (i.e., double peaks)  
244 that were coded as ambiguous characters between the two corresponding nucleotides. To consider this  
245 variation in the analyses, we used the program Phase v.2.1 ([Stephens & al., 2001](#)), which has been proven  
246 a useful tool in other studies (e.g., [Ronikier & al., 2012](#)). This software allows the inference of different  
247 coexisting alleles per individual. However, as a limitation, it assumes that a maximum of two alleles are  
248 present in one individual. This is not necessarily the case for ribosomal DNA, which has multiple copies  
249 in the genome. The ETS dataset was composed of 159 specimens of the *H. pendulum* complex together  
250 with 36 specimens representing the remaining species of sect. *Stoechadina*. The web tool Seqphase  
251 (<http://seqphase.mpg.de/seqphase/>) was used to generate the Phase input files from the fasta sequence  
252 alignments and later to convert the Phase output files back into fasta. Using this ETS dataset and the  
253 *rpl32-trnL* dataset, a network of ribotypes/haplotypes was constructed using the statistical parsimony  
254 algorithm ([Templeton & al., 1992](#)) implemented in the TCS v.1.21 software ([Clement & al., 2000](#)) with  
255 95% confidence limits. In these analyses, for both markers, indels were coded as discrete characters using  
256 the modified complex indel coding method implemented in SeqState v.1.4.1 ([Müller, 2006](#)).

257 Phylogenetic relationships among the different haplotypes and ribotypes of the complex found in  
258 the TCS analyses were inferred separately using four additional species in the case of *rpl32-trnL*—*H.*  
259 *arvae* J. R. I. Wood, *H. marginatum* DC., *H. monogynum* B. L. Burt & Sunding and *H. montanum*

260 DC.—and two species in the case of ETS—*H. gossypinum* Sch. Bip. and *H. orientale* (L.) Gaertn.—  
261 which were used as outgroup taxa based on previous studies (Galbany-Casals & al., 2014). With these  
262 two datasets—dataset 1 (*rpl32-trnL*) and dataset 2 (ETS)—Bayesian inference (BI) and Maximum  
263 Parsimony (MP) phylogenetic analyses were performed separately. Bayesian inference analyses were  
264 conducted with MrBayes v.3.1.2 (Ronquist & Huelsenbeck, 2003). The best-available model of molecular  
265 evolution was selected using the Akaike information criterion as implemented in jModel-Test v.0.0.1  
266 (Posada, 2008). For *rpl32-trnL* and ETS, the best fitting models were GTR+G and GTR+I+G,  
267 respectively. In accordance with the MrBayes manual, we used the restriction model (F81) for the indel  
268 partition of both regions. Two simultaneous and independent analyses of four Metropolis-coupled Markov  
269 chains were run for 5 million generations, starting from different random trees and saving one every 500  
270 generations. After checking the analysis performance and the effective sample size values (ESS) with  
271 Tracer v.1.6.0 (Rambaut & al., 2013), the first 25% of the trees of each analysis were discarded (burn-in).  
272 A 50% majority-rule consensus tree was computed with MrBayes for the remaining trees and was  
273 visualized with FigTree v.3.1 (Rambaut, 2009). Maximum parsimony bootstrap analyses (Felsenstein,  
274 1985) were performed with PAUP v.4.0b10 (Swofford, 2002) with 1000 replicates, random taxon addition  
275 with 10 replicates, and no branch swapping. Parsimony uninformative characters were excluded to  
276 standardize the parsimony statistics.  
277

278 **Geographic structure analyses.** — The geographic structure of genetic variation was assessed  
279 by analyses of molecular variance (AMOVA) following the approach of Excoffier & al. (1992) using the  
280 programme Arlequin v.3.5.1.2 (Excoffier & al., 2005). AMOVAs were performed at different hierarchical  
281 levels: (1) treating all populations as a single group to determine the percentage of variation between and  
282 within populations; (2) dividing populations into two groups: the western group (Majorca, Ibiza,  
283 Vedranell, Es Vedrà, Alicante, Gibraltar, Morocco and Algeria) and the central group (Sardinia,  
284 Marettimo, Pantelleria, Malta), to determine the percentage of variation accounting for differences  
285 between the western and central groups, between populations within groups and within populations; and  
286 (3) grouping populations according to smaller geographical areas, mostly corresponding to islands or  
287 areas showing discontinuity with others (Majorca, Imperialet, Ibiza, Vedranell, Es Vedrà, Alicante,  
288 Gibraltar, Morocco, Algeria, Sardinia, Sicily, Marettimo, Pantelleria and Malta) to determine the  
289 percentage of variation attributable to differences between the geographical groups, between populations  
290 within groups and within populations. The significance levels of the variance components were obtained  
291 by a nonparametric test using 1023 permutations. Phylogeographical structure was also investigated by  
292 the Bayesian clustering method implemented in BAPS v.6.0 (Corander & al., 2008), choosing a spatial  
293 clustering algorithm with an unlikage model among polymorphic sites, and a mixture analysis of  
294 individuals with geographic information. We ran 10 replicates from each of the nine simulations from  $K =$   
295  $2$  to  $K = 10$ . The most likely  $K$  was chosen according to the highest log marginal likelihood [log (ml)]  
296 values. We used Barrier v.2.2 (Manni & al., 2004) to identify where possible barriers to gene flow  
297 between *H. pendulum* populations could exist. Monmonier's maximum difference algorithm was applied  
298 on Nei genetic distances (Nei, 1972) obtained from GenAlEx v.6.5 (Peakall & Smouse, 2012).  
299 Geographical coordinates of populations were used to obtain a Voronoï tessellation of the study area, on  
300 which the five strongest putative barriers were delineated.  
301

302 **Phylogenetic relationships with other species of the genus and the effects of**  
303 **hybridization.** — We also aimed to examine the phylogenetic relationships between the *H. pendulum*  
304 complex and other species of the genus and to identify possible ancient hybridization events. To achieve  
305 these goals, the different haplotypes and ribotypes found in the *H. pendulum* complex were added to a  
306 broader sampling of congeneric species of *rpl32-trnL* (dataset 3) or ETS (dataset 4) sequences. Taxa were  
307 selected based on previous work (Galbany-Casals & al., 2009, 2014). Dataset 3 included a broad  
308 sampling of the Mediterranean-Macaronesian-Asiatic clade, including all species of sect. *Stoechadina*.  
309 Dataset 4 included all ribotypes retrieved with Phase in members of sect. *Stoechadina* (see above). In  
310 both cases, several regions that could not be aligned were manually excluded. Indels were treated as for  
311 network representation (see above). With these two datasets, BI and MP analyses were performed as

described above using *H. argyrosphaerum* DC. and *H. litorale* H. Bol. as outgroup taxa for *rpl32-trnL*, and *H. gossypinum* and *H. orientale* in the case of ETS, based on Galbany-Casals & al. (2014). The best fitting model of molecular evolution was GTR+G+I for both markers. Additionally, using the same software and conditions described above, we constructed an additional parsimony network for *rpl32-trnL* that included the 15 haplotypes of the *H. pendulum* complex and members of the Mediterranean-Macaronesian-Asiatic clade. Finally, a neighbour-net (NN) analysis was conducted for ETS using SplitsTree4 v.4.10 (Huson & Bryant, 2006) with default options including all ribotypes found in the *H. pendulum* complex and in the other species of sect. *Stoechadina*.

**Morphology.** — The pattern of morphometric variation within sect. *Stoechadina* and within the *H. pendulum* complex was evaluated based on 31 characters (Table 1) that were recognized as taxonomically relevant in previous studies (Galbany-Casals & al., 2006a) or that appeared to be variable during the course of the present study (S. Herrando, pers. obs.). Involucral bracts, florets and indumentum were examined under a ZEISS Stemi DV4 binocular stereoscopic microscope. The characters used for each multivariate analysis, the characters measured, and the type of each character (quantitative, qualitative or semiquantitative) are specified in Table 1. For the quantitative and semiquantitative characters, the mean of three to five measurements per specimen was used in the analyses.

Exploratory PCAs were performed using individuals as operational taxonomic units. Although some authors discourage the use of non-quantitative data, the basic objective of PCA—to summarize most of the ‘variation’ that is present in the original set of  $p$  variables using a smaller number of derived variables—can be achieved regardless of the nature of the original variables (Jolliffe, 2002). A first multivariate analysis (PCA1) was conducted to examine the morphological variability across the whole of sect. *Stoechadina* and the morphological distinction of the *H. pendulum* complex. Based on the results of PCA1 (see Results), an additional analysis excluding *H. heldreichii* Boiss. and members of the *H. italicum* (Roth) G. Don complex was performed (PCA2) in order to reduce the influence of the morphological variability of these taxa in the extraction of the morphological variation of the rest of taxa, which included the *H. pendulum* complex members, *H. stoechas* and *H. crassifolium*. The next analysis (PCA3) was aimed at evaluating the morphological variation within the *H. pendulum* complex, as well as analysing the consistency of previously recognized taxa. To ease the evaluation of the morphological congruence of the existing taxonomic treatments with PCA, the individuals were labelled in the scatterplots according to predefined groups. We considered the following 11 taxa: *H. boissieri* Nyman, *H. errerae* var. *errerae*, *H. errerae* var. *messerii* (Pignatti) Raimondo, *H. fontanesii* Cambess., *H. hyblaeum* Brullo, *H. melitense*, *H. nebrodense* Heldr., *H. panormitanum* Guss., *H. pendulum*, *H. saxatile* Moris and *H. valentinum*. Next, integrating morphological patterns visualized in the PCA3 with information obtained from the genetic variation of the group, we considered that five potential species could be recognized within the complex: *H. errerae*, *H. melitense*, *H. pendulum*, *H. saxatile* and *H. valentinum*. Considering these five taxa, we performed a CDA that, maximizing the discrimination among groups, shows whether predefined groups of species may be distinguishable based on measured characters and which characters contribute to their separation. Binary variables were not used in these analyses given that they were constant within groups. Additionally, *H. valentinum* and *H. saxatile* were analysed with the putative parental species, *H. pendulum* and *H. stoechas* (PCA4), and *H. pendulum* and *H. italicum* (PCA5), respectively, to test their plausible hybrid origin based on our molecular results and previous morphological observations (Galbany-Casals & al., 2006a). Two characters—presence or absence of succulent leaves and synflorescence density—were excluded from these last two analyses because they were not relevant to the taxa involved.

Finally, differences in morphological traits studied in the five taxa accepted here were tested for significance to identify diagnostic characters. First, each morphological character was evaluated to verify the normality requirement. Characters that followed a normal distribution were tested by one-way analyses of variance (ANOVA) in conjunction with Tukey’s *post hoc* multiple comparisons test. The characters that did not meet the normality requirement were log-transformed. When the log-transformed variables were normally distributed, ANOVAs were performed as described above. For characters for which the transformation did not improve the distribution, pairwise Kruskal-Wallis tests were performed

364 using Bonferroni correction for multiple comparisons. All comparisons of means were performed using  
365 the mean value for each character and specimen. The morphometric study was conducted using SPSS  
366 v.17.0 (SPSS Inc., Chicago, IL, USA).

367  
368

## 369 ■ RESULTS

370

371 **Network representation and phylogenetic analyses.** — The *rpl32-trnL* and the ETS  
372 sequences for the *H. pendulum* complex ranged from 855 to 870 bp (with a total aligned length of 927 bp  
373 including indels) and from 880 to 884 bp (with a total aligned length of 884 bp), respectively.

374 A total of 15 cpDNA haplotypes were identified in the *H. pendulum* complex (Figs. 1A, 1B; Electr.  
375 Suppl.: Table S1). The most widely distributed haplotype was H1 (65.3% of all samples), whereas  
376 haplotypes H6, H7 and H8 were only found in one individual (Fig. 1A; Electr. Suppl.: Table S1). In most  
377 populations, a single haplotype was sampled. Only ten of the 44 populations contained several  
378 haplotypes, and seven of them contained one private haplotype. Although some haplotypes were species-  
379 specific, others were shared by different taxa (Fig. 1B; Electr. Suppl.: Table S1). Three main groups of  
380 haplotypes were detected, and they were separated from one another by at least nine mutational steps:  
381 H1–H8, H9 and H10–H15 (Fig. 1A; Electr. Suppl.: Fig. S1). In the H1–H8 group, seven haplotypes were  
382 derived from one dominant haplotype (H1) by one or two mutational steps. In contrast, group H10–H15  
383 contained more divergent haplotypes.

384 In the case of ETS, among all 159 individuals sequenced, 41 contained additive polymorphic sites.  
385 For these individuals a double sequence was generated using the Phase software. Similarly, 10 specimens  
386 of the other species of sect. *Stoechadina* also contained double peaks, and thus several coexisting  
387 ribotypes were also recovered with the Phase software. As a result, we finally obtained 200 ETS  
388 sequences for the *H. pendulum* complex and 46 sequences for the remaining species of sect. *Stoechadina*.  
389 Among these sequences, 72 nrDNA ribotypes were identified for the *H. pendulum* complex (Fig. 2A), and  
390 38 nrDNA ribotypes were obtained for the other taxa of sect. *Stoechadina* (Electr. Suppl.: Table S1). In  
391 general, there were no shared ribotypes between different taxa of the complex, except for ribotypes R34,  
392 R55, R56 and R62 (Fig. 2A; see details in Electr. Suppl.: Table S1, Fig. S2). There were also no shared  
393 ribotypes between members of the *H. pendulum* complex and other species of sect. *Stoechadina* (Electr.  
394 Suppl.: Table S1, Fig. S3). Coexisting ribotypes in one individual grouped together in a well-supported  
395 clade in 41.5% of the cases, whereas in the remaining cases the different ribotypes found in one  
396 individual were not grouped together (Electr. Suppl.: Table S1, Fig. S2). Noticeably, coexisting ribotypes  
397 detected in five individuals of *H. saxatile* were placed in different supported clades: ribotypes R62/R65  
398 detected in one individual of population S1, ribotypes R64/R66 and R62/R66 detected in two individuals  
399 from S3, and ribotypes R61/R67 and R63/R66 detected in two individuals from S4 (Electr. Suppl.: Fig.  
400 S2). In almost half of the populations (21) intraindividual variation was detected. In 14 populations, a  
401 single ribotype was sampled, whereas 30 populations were polymorphic. Only two populations were  
402 homogeneous for a private ribotype (R17 from population F11 and R19 from F4). Many ribotypes were  
403 found in only one individual (41 ribotypes). The most widely distributed ribotype was R18 (8.5% of all  
404 samples), and only four ribotypes exceeded a frequency of 5% (R18, R25, R56, R68; Electr. Suppl.: Table  
405 S1). To simplify the geographical representation of the ribotypes, they were classified into 18 groups (Fig.  
406 2A) based on the phylogenetic relationships obtained in the BI and MP analyses (Electr. Suppl.: Fig. S2).  
407 Three supported clades were recovered in BI and MP phylogenetic analyses: one clade comprised  
408 ribotypes R1–R9 (PP = 0.97; Electr. Suppl.: Fig. S2), which are distributed in the central Mediterranean  
409 area, specifically in Algeria, Malta and Sicily; a second clade was composed of ribotypes R10–R43 (PP =  
410 0.97; Electr. Suppl.: Fig. S2), which are found in the western part of the Mediterranean Basin, specifically  
411 in the Iberian Peninsula, Majorca, Ibiza, Morocco and Algeria; and the third well supported clade  
412 comprised ribotypes R54 to R72 from Sicily, Pantelleria and Sardinia (PP = 1, BS = 87; Electr. Suppl.:  
413 Fig. S2). The position of the remaining ribotypes (from several locations both in western and central  
414 Mediterranean areas) was not resolved.

415



416 **Geographical structure analyses.** — In the AMOVA, approximately 87.3% of the *rpl32-trnL*  
417 variation in the *H. pendulum* complex was explained by differences between populations when no  
418 regional differentiation was considered, whereas 66.9% was explained by differences among restricted  
419 geographical groups when regional differentiation was hypothesized (Table 2). In the case of ETS,  
420 although most of the variation (83.9%) could be attributed to differences between populations, a  
421 significant percentage of the variation was due to differences between the western and central groups  
422 (54.6%), and between more restricted geographical groups (58.2%), supporting the presence of  
423 phylogeographical structure for this marker.

424 BAPS analyses identified  $K = 2$  ( $\log(\text{ml}) = -9745.1$ ) for *rpl32-trnL* data and  $K = 6$  ( $\log(\text{ml}) =$   
425  $-2187.3$ ) for ETS data as the optimal number of genetically homogeneous groups (Figs. 3A, 3B). In the  
426 Barrier analysis, the first genetic barrier was inferred between Malta and the remaining populations in the  
427 case of *rpl32-trnL* (Fig. 3C), or between western and central Mediterranean populations in the case of  
428 ETS (Fig. 3D).

429  
430 **Phylogenetic relationships with other species of the genus and the effects of**  
431 **hybridization.** — In the *rpl32-trnL* analyses, the phylogram showed a supported Mediterranean-  
432 Macaronesian-Asiatic clade (BS = 94, PP = 1; Fig. 1D). It was divided into three subclades (coloured in  
433 blue, pink and yellow), which were not correlated with classification at the species, the complex or the  
434 sectional level, and none of which had geographical structure. Individuals of the *H. pendulum* complex  
435 and *H. stoechas* were found in each of the three subclades, and *H. italicum* and *H. serotinum* Boiss. had  
436 individuals in two of the three subclades. The statistical parsimony analysis provided the network shown  
437 in Fig. 1C, where three main groups, corresponding to the three subclades recovered in Fig. 1D, are  
438 coloured. The yellow group is separated from the other two by three mutational steps, and the blue and  
439 the pink groups are six mutational steps apart (Fig. 1C). In the ETS analysis, the *H. pendulum* complex  
440 was not monophyletic (Electr. Suppl.: Fig. S3). Furthermore, none of the other species of sect.  
441 *Stoechadina* represented by several individuals was monophyletic (Electr. Suppl.: Fig. S3). In the NN  
442 analysis and the phylogenetic analysis (Fig. 2B and Electr. Suppl.: Fig. S3), ribotypes R54–R72 were  
443 closely related to *H. litoreum* Guss., *H. italicum* subsp. *italicum*, *H. italicum* subsp. *microphyllum* (Willd.)  
444 Nyman, *H. italicum* subsp. *tyrrhenicum* (Bacch., Brullo & Giusso) Herrando, J.M. Blanco, L. Sáez &  
445 Galbany and *H. massanellanum* Herrando, J.M. Blanco, L. Sáez & Galbany, while the remaining  
446 ribotypes (R1 to R53) were more related to *H. stoechas*, *H. heldreichii*, *H. crassifolium* and *H. serotinum*  
447 Boiss. Ribotypes from western locations were closely related to the specimens of *H. stoechas* sampled in  
448 geographically close localities (Iberian Peninsula and Ibiza), whereas ribotypes from southern Sicily,  
449 eastern Algeria and Malta were grouped with specimens of *H. stoechas* from the eastern Mediterranean  
450 area (Crete, Greek Islands and Tunisia). Ribotypes found in *H. valentinum* were closely related to *H.*  
451 *stoechas*, one of its putative progenitors. The ribotypes found in *H. saxatile* also were genetically close to  
452 one of the plausible parental species, *H. italicum*.

453  
454 **Morphology.** — PCA1 revealed two main groups within sect. *Stoechadina*: one was composed of  
455 members of the *H. italicum* complex and *H. heldreichii*, and the other consisted of the *H. pendulum*  
456 complex, *H. stoechas* and *H. crassifolium* (Electr. Suppl.: Fig. S4A). Characters that mainly contributed  
457 to the separation of these two groups on the first axis (38.3% of total variance) were width of the  
458 outermost involucre bract and total number of florets per capitulum, both of which were higher in the  
459 second group. The second analysis (PCA2) was focused on the second group only. The first axis  
460 accounted for 20.7% of the total variation, and the second axis accounted for 14.3%. In this case, *H.*  
461 *crassifolium* and *H. stoechas* were separated from the *H. pendulum* complex mainly due to higher  
462 synflorescence length values and the presence of succulent leaves in *H. crassifolium* and leaves with a  
463 denser glandular indumentum on the abaxial side in *H. stoechas* (Electr. Suppl.: Fig. S4B).

464 In the PCA3 analysis, the first axis accounted for 16.4% of the total variation and the second axis  
465 accounted for 16.2%. Although these values may look low, they are well above the limits computed by  
466 the broken stick rule, which mark the lower limit below which a given axis should be considered to  
467 explain random variation (in this case, for the given number of variables: 13.0%, 9.8%, 8.2%, and 7.1%

468 for the first four axes). The graphical representation (Fig. 4A) showed a main cloud with a broad range of  
469 variation and four satellite units. The central cloud was formed by specimens of several taxa—*H.*  
470 *boissieri*, *H. errerae* var. *messerii*, *H. fontanesii*, *H. hyblaenum*, *H. nebrodense*, *H. panormitanum* and *H.*  
471 *pendulum*—with a large amount of overlap. Around this main cloud, four different entities were observed  
472 that corresponded to *H. errerae* var. *errerae*, *H. melitense*, *H. saxatile* and *H. valentinum*. Considering all  
473 combinations of the first four axes, *H. melitense* and *H. errerae* var. *errerae* were recovered as well  
474 separated taxa, whereas there was more overlap among the remaining three taxa (*H. saxatile*, *H.*  
475 *valentinum* and *H. pendulum*; Electr. Suppl.: Fig. S5).

476 The CDA plot showed that the individuals in the *H. pendulum* complex were distributed in three  
477 main clouds (Fig. 4B). One was composed of the specimens of *H. errerae*, constituting the most  
478 differentiated group, which was isolated from the remaining specimens along the first axis accounting for  
479 66.2% of the total variation. The characters that correlated with the first canonical axis and were thus  
480 responsible for the separation of *H. errerae* were mostly outermost involucre bract texture, number of  
481 hermaphroditic florets per capitulum and width of the outermost involucre bract. The following cloud,  
482 which differed noticeably from the others along the third axis (explaining 12.3% of variation), was  
483 composed of individuals of *H. melitense*, and features that contributed to its differentiation were  
484 capitulum width, capitulum length and capitulum length/capitulum width. The remaining individuals of  
485 the complex were grouped in a third group composed of *H. saxatile*, *H. valentinum*, and *H. pendulum*,  
486 among which the latter showed the highest intragroup variation. Although these species showed some  
487 overlap, they were distributed along the second axis, which correlated with the total number of florets per  
488 capitulum, capitulum width and capitulum length/capitulum width. However, this axis only accounted for  
489 13.8% of the total variance. The total percentage of correctly classified individuals in these five  
490 predefined groups was 97.8%. All *H. errerae* and *H. melitense* individuals were correctly classified,  
491 whereas the percentages of correctly classified specimens for the other taxa were: 92.3% for *H. saxatile*,  
492 96.4% for *H. valentinum* and 98.8% for *H. pendulum*. Misclassified specimens of *H. saxatile* and *H.*  
493 *valentinum* were classified as *H. pendulum*, and misclassified specimens of *H. pendulum* were classified  
494 as *H. valentinum*.

495 In PCA4, the first principal component showed that *H. valentinum* was placed in an intermediate  
496 position between *H. pendulum* and *H. stoechas* in terms of their scores for that component, although with  
497 a considerable degree of overlap among them (Fig. 5A). *Helichrysum saxatile* displayed a similar  
498 morphological transition, located between *H. pendulum* and *H. italicum* in PCA5 along the first  
499 component (Fig. 5B). However, in that case, *H. saxatile* was clearly placed closer to one of its putative  
500 parents, *H. pendulum*.

501 Finally, the comparison of means (Electr. Suppl.: Table S2) showed that *H. errerae* differed  
502 significantly ( $p < 0.05$ ) from the other taxa by having narrower outermost involucre bracts that are  
503 completely to partially herbaceous and tomentose rather than papery and glabrous. *Helichrysum melitense*  
504 has succulent leaves—unlike the remaining species within the complex—and wider innermost involucre  
505 bracts. *Helichrysum saxatile* showed significant differences in comparison to the others, excluding *H.*  
506 *errerae*, with fewer pistillate and hermaphroditic florets per capitulum and shorter outermost involucre  
507 bracts. Regarding *H. valentinum*, a higher density of glandular hairs on the abaxial side of the leaves and  
508 fewer capitula per synflorescence accounted for most of its differentiation from the other taxa. Finally, *H.*  
509 *pendulum* showed the greatest variation for a greater number of the characters analysed, although that  
510 species is characterized by a less dense eglandular indumentum on the adaxial side of the leaves  
511 compared with *H. melitense* and *H. saxatile*, and a larger number of involucre bracts per capitulum than  
512 *H. valentinum*.

## 514 ■ DISCUSSION

515

516 **Phylogeographic history of the *Helichrysum pendulum* complex.** — Our results revealed  
517 high values for haplotype (4) and ribotype (21) diversity in northern Africa, together with a large number  
518 of private haplotypes (3) and ribotypes (19), potentially supporting a northern Africa origin of the

519 complex (Figs. 1B, 2A; Electr. Suppl.: Table S1). Sicily stood out to be the second region with high  
520 levels of haplotype (5) and ribotype (14) diversity, but haplotypes from Sicily belong all to only one of  
521 the three main groups retrieved by cpDNA data, in contrast with the haplotypes found in northern Africa,  
522 that correspond to the three different groups (Fig. 1A, coloured groups/clades in Figs. 1C, 1D). Previous  
523 studies have strongly suggested an African origin for the whole Mediterranean-Macaronesian-Asiatic  
524 clade of *Helichrysum*—including sect. *Stoechadina* and the *H. pendulum* complex—ca. 5 Ma ago  
525 (Galbany-Casals & al., 2009, 2014). Despite this evidence, the resolution obtained in the present study in  
526 both the nrDNA and the cpDNA phylogenetic trees is not sufficient to infer the geographic origin of the  
527 *H. pendulum* complex with confidence (Electr. Suppl.: Figs. S1, S2). In addition, it must be noted that  
528 other authors, such as Petit & al. (2003), have demonstrated that the highest diversities can represent  
529 contact zones rather than areas of origin. In fact, this may be, at least in part, the case for the *H. pendulum*  
530 complex, given that Moroccan and Algerian populations are placed in an area with high reticulation in the  
531 NN graphic (Fig. 2B).

532 In the unique dated phylogeny including Mediterranean *Helichrysum*, the clade comprising the  
533 whole Mediterranean-Macaronesian-Asiatic clade of *Helichrysum* and the genus *Anaphalis* had a  
534 divergence time estimation of 7.04 (5.45-8.89) Ma (Nie & al., 2016). This was the closest supported dated  
535 node to sect. *Stoechadina* clade, which is included within the Mediterranean-Macaronesian-Asiatic clade  
536 and would then be younger. However, no members of the *H. pendulum* complex were included in this  
537 work. For this reason, the temporal origin of the *H. pendulum* complex cannot be determined with  
538 precision at the moment. With this approximate temporal framework, the ancestors of the complex could  
539 have expanded across the western and central Mediterranean regions during times of reduced distances  
540 between islands and continental landmasses, either during the MSC or the Pleistocene glaciations.  
541 Establishment of the Mediterranean climate with dry summers (3.2 Ma) and Quaternary oscillations with  
542 glacial and interglacial stages (from 2.3 Ma to present) may also have promoted diversification driven by  
543 isolation in reduced areas, causing allopatric speciation (e.g., Blanco-Pastor & al., 2012). Additionally,  
544 long-distance dispersal events, favoured by the putative excellent dispersal ability of the tiny achenes (~1  
545 mm), are the most plausible explanation for the complex expansion to areas isolated by the sea, e.g., the  
546 Balearic Islands, which have remained isolated since the opening of the Gibraltar Strait (5.3 Ma;  
547 Thompson, 2005). The maintenance of this sea mass along the longitudinal axis of the Mediterranean  
548 Basin, even during Pleistocene glaciations, caused east-west phylogeographical breaks, which have been  
549 detected in many plant groups (Nieto-Feliner, 2014). The *H. pendulum* complex is one of these cases, as  
550 supported by nrDNA data (Fig. 3D). A moderately high percentage of the variation was observed between  
551 the western and central groups (54.6%; Table 2) which share a small number of ribotypes (Fig. 2A; Electr.  
552 Suppl.: Table S1). The general distribution of ribotypes revealed a high level of genetic similarity  
553 between plants from geographically close localities (Fig. 2A), suggesting an increased probability of  
554 genetic exchange among neighbouring populations. A similar pattern was also detected in a  
555 phylogeographic study of the Mediterranean *H. italicum* (Galbany-Casals & al., 2011), for which the  
556 importance of gene flow and genetic affinities among neighbouring populations was highlighted. A high  
557 level of genetic differentiation between populations found in the AMOVA (87.3% for *rpl32-trnL*, 83.8%  
558 for ETS, Table 2) is likely a consequence of the habitat of these species, given that strong discontinuities  
559 between cliff areas contribute to progressive reproductive isolation between populations (Thompson,  
560 2005).

561 Both markers revealed a strong genetic differentiation of the Maltese populations (considered here  
562 as *H. melitense*), which are characterized by the presence of an exclusive haplotype (H15) separated by  
563 seven mutational steps from the closest haplotype (Fig. 1A) and a unique set of ribotypes (R1 and R2,  
564 Fig. 2). Additionally, the first genetic barrier for cpDNA was detected between Malta and the remaining  
565 populations (Fig. 3C). These results are consistent with the detection of unique haplotypes in Maltese  
566 populations of *Anthemis secundiramea* Biv. (Lo Presti & Oberprieler, 2011). Our results could suggest  
567 an ancient colonization of Malta by seeds, followed by genetic drift due to the long isolation of the  
568 archipelago from other regions. The NN graphic (Fig. 2B) and the supported clade recovered from the  
569 nrDNA data (PP = 0.97; Electr. Suppl.: Fig. S2) revealed genetic affinities between the *H. pendulum*  
570 complex populations from southern Sicily, Algeria and Malta. The affinities between the Maltese and the  
571 Sicilian flora and fauna have been well documented (Junikka & al., 2006) and have been attributed to

572 gene flow during Quaternary glaciations when the sea level fell. Currently, *H. melitense* remains restricted  
573 to the western cliffs of Gozo Island, covering an area of less than 25 km<sup>2</sup>, and they are probably extinct  
574 from Malta Island (Sciberras & Sciberras, 2009).

575 In contrast to the high genetic differentiation of *H. melitense*, we observed low levels of genetic  
576 diversity in *H. errerae* populations from Pantelleria, in agreement with the recent emergence of  
577 Pantelleria Island dated to 114 000 years ago (Wallmann & al., 1988), entailing a recent origin for this  
578 taxon that probably resulted from a long-distance seed dispersal event. Since its formation, Pantelleria has  
579 never been connected to Sicily or Tunisia. However, during the Last Glacial Maximum (19,000–22,000  
580 years ago; Yokoyama & al., 2000), Pantelleria was separated from Sicily only by a narrow strait (Lo  
581 Presti & Oberprieler, 2011), which could have favoured gene flow between Sicily and the Pantelleria  
582 populations. In fact, the phylogenetic affinities of *H. errerae* ribotypes to one *H. pendulum* ribotype  
583 detected in southern Sicily (R70) (Fig. 2) suggest a Sicilian origin for *H. errerae*. However, the two  
584 exclusive ribotypes detected in Pantelleria (R68 and R69) indicate the current genetic isolation of these  
585 populations, in agreement with a notable morphological differentiation from *H. pendulum* and a local  
586 adaptation to distinct habitat conditions, i.e., volcanic rocks rather than limestone substrates (M. Galbany-  
587 Casals, pers. obs.).

588 The geographic proximity of landmasses on both sides of the Strait of Gibraltar appears to have  
589 played a significant role allowing the genetic exchange between populations in the *H. pendulum* complex.  
590 In particular, our results show a haplotype (H10) that is shared between populations on both sides of the  
591 strait (Fig. 1B), suggesting the occurrence of gene flow as described for other plant groups (e.g., Ortiz &  
592 al., 2007; Arroyo & al., 2008). These results may indicate an ancient expansion of the *H. pendulum*  
593 complex by seeds across the Gibraltar Strait. Haplotype H10 is an internal haplotype, which led us to  
594 support this plausible scenario. Although gene flow has been effective in the past between populations of  
595 *H. pendulum* on both sides of the Strait, our data also suggest that dispersal and gene exchange were  
596 subsequently hindered, resulting in the recent genetic differentiation of the two populations. In particular,  
597 no ribotypes are shared between the Gibraltar (Iberian Peninsula) and Rif (Moroccan) populations,  
598 indicating a lack of pollen or seed exchange. Moreover, the Gibraltar population contains an exclusive  
599 haplotype (H11) that is not present in the Rif population, whereas the Rif population contains five  
600 different ribotypes, four of which are exclusive to that population. The exclusive markers found in both  
601 populations indicate that they have been sufficiently isolated to become differentiated from one another  
602 and from surrounding populations on their side of the Strait. This pattern resembles the one recovered for  
603 *Quercus ilex* L. (Lumaret & al., 2002) and is similar to that of *Laurus nobilis* L. (Rodríguez-Sánchez &  
604 al., 2008). The genetic differentiation of populations from the Strait of Gibraltar, both from one another  
605 and from surrounding populations on the same side of the Strait, has been interpreted to reflect the role of  
606 the areas close to the Strait of Gibraltar as a glacial refuge (Rodríguez-Sánchez & al., 2008).

607 Regarding the role of the Sicilian Strait, the NN analysis (Fig. 2B) shows a genetic affinity  
608 between populations from southern Sicily and eastern Algeria. The larger number of ribotypes found in  
609 North African populations (in comparison to Sicilian ones) might indicate the direction of gene flow from  
610 Algeria towards Sicily, as suggested for other plant groups (e.g., Hilpold & al., 2011; Lo Presti &  
611 Oberprieler, 2011), although this is difficult to assure based on the present data. The genetic similarities  
612 between populations in eastern Algeria and southern Sicily could be explained by land connections during  
613 the MSC (Rosenbaum & al., 2002) or by dispersal events. In the latter, both occasional long-distance  
614 dispersal (Cowie & Holland, 2006; Fernández-Mazuecos & Vargas, 2011) and/or stepping-stone dispersal  
615 through emerged islands during low sea level periods (Stöck & al., 2008) could occur.

616  
617 **Evidence of past hybridization in the *Helichrysum pendulum* complex.** — The lack of  
618 concordance between the cpDNA and nrDNA markers, and between the cpDNA and taxa delimitation, is  
619 remarkable (Figs. 1, 2). Although the use of a single chloroplast marker may seem somewhat limited, we  
620 found a reasonable degree of variability and a complex pattern of variation. For these reasons, incomplete  
621 sampling of cpDNA markers does not seem to be the cause of incongruence between cpDNA and nrDNA.  
622 In particular, we detected a sharing of—or grouping of closely related—cpDNA haplotypes by different  
623 species. Similar patterns have also been detected in other plant groups (e.g., Comes & Abbott, 2001;  
624 Smissen & al., 2004; Lo Presti & Oberprieler, 2011; Zozomová-Lihová & al., 2014). Although selection,

625 recombination, homoplasy (convergent evolution) and gene duplication (paralogy) have been reported as  
626 possible causes of incongruence between cpDNA and nrDNA data (Wendel & Doyle, 1998), two  
627 evolutionary processes, which are not mutually exclusive, remain the main hypotheses explaining these  
628 types of gene incongruences: (1) horizontal transfer of genes via hybridization and introgression (ancient  
629 or recent); and/or (2) persistence of ancestral polymorphisms through multiple speciation events  
630 (incomplete lineage sorting (ILS) or deep coalescence). The distinction between these two processes might  
631 represent a problem that is too difficult to resolve analytically, and a widely applicable approach to do this  
632 does not yet exist. The sharing of haplotypes among allopatric taxa could be an argument to support  
633 retention of polymorphisms rather than hybridization. For example, haplotype H9 from Algeria was  
634 grouped with geographically and taxonomically distant specimens of *H. italicum* subsp. *tyrrhenicum* from  
635 Dragonera (Balearic Islands) and *H. rubicundum* (K. Koch) Bornm. from Iran, with the latter belonging to  
636 sect. *Helichrysum* Mill. (Fig. 1). However, phenomena such as migration and range contraction could also  
637 explain this pattern. Additionally, ILS is less likely to occur in plastid compared with nuclear genomes  
638 due to its small effective population size.

639 In *Helichrysum*, previous work documented a high level of cpDNA variation in a network  
640 representation of the haplotypes found in the *H. italicum* complex, in which three markedly distinct  
641 groups of haplotypes were detected (Galbany-Casals & al., 2011). However, that study only included  
642 members of the *H. italicum* complex, thus the possibility that part of such variability could be due to  
643 hybridization with other groups was not explored. In the present study, we recovered the same three main  
644 groups of haplotypes (Figs. 1C, 1D, three different background colours), each of which was composed of  
645 a mixture of taxa. A careful examination of relationships among taxa within each haplotype group can  
646 provide some insights into the underlying processes. In most cases, the obtained pattern highlights past  
647 hybridization events, as reported for other plant groups (Jackson & al., 1999; Fehrer & al., 2007; Blanco-  
648 Pastor & al., 2012).

649 The first case of possible past hybridization was detected between populations of the *H. pendulum*  
650 complex and the *H. italicum* lineage (Figs. 1C, pink group; 1D, pink-shaded clade). The present-day set of  
651 haplotypes H10–H15 would derive from the *H. italicum* lineage, which would have donated its  
652 chloroplast genome and acted as maternal parent. At least three independent chloroplast capture events  
653 would have occurred: the first one would explain the presence of haplotypes H10 and H11 in North  
654 African and South Iberian populations of *H. pendulum*, with no consequences for the morphological  
655 differentiation of these populations; the second one would explain the presence of haplotypes H12–H14  
656 in populations from Sardinia, which are treated here as *H. saxatile*. In this case, the close relationships of  
657 ribotypes R60–R67 found in *H. saxatile* with ribotypes found in members of the *H. italicum* complex also  
658 support this hypothesis (Fig. 2). This relationship is also supported by the morphometric analysis, in  
659 which *H. saxatile* showed an intermediate morphology between *H. pendulum* and *H. italicum* (Fig. 5B).  
660 The third one would explain the presence of H15 in populations from Malta, which are considered here as  
661 *H. melitense*. Three factors favour past hybridization events over current gene flow: (1) the haplotypes of  
662 *H. saxatile* and *H. melitense* are closely related to certain *H. italicum* haplotypes (Figs. 1C, 1D), but not  
663 identical as they are expected to be in case of recent or current gene flow; (2) no ribotypes are shared  
664 between *H. melitense* or *H. saxatile* and *H. italicum* and only one ribotype of *H. saxatile* is shared with  
665 *H. pendulum* (Fig. 2B; Electr. Suppl.: Fig. S3); and (3) *Helichrysum saxatile* and *H. melitense* are  
666 morphologically differentiated from *H. pendulum* and *H. italicum* (Figs. 4-6; Electr. Suppl.: Fig S4).  
667 These data clearly suggest that chloroplast capture was a past event and was followed by isolation and  
668 subsequent genetic and morphological differentiation in the respective islands. Past interspecific  
669 hybridization within *Helichrysum* has been suggested in previous studies (Galbany-Casals & al., 2009,  
670 2014). The finding that *H. italicum* is not currently present in Malta further supports the hypothesis of  
671 past gene flow over current hybridization; as discussed above, both migration or range contraction could  
672 explain the possibility of past gene flow between currently allopatric taxa.

673 A second case of possible past hybridization is that involving the origin of *H. valentinum*. This  
674 taxon shows a notable variation in ribotypes. Whereas ribotype R34 is shared with *H. pendulum*, the two  
675 divergent ribotype groups R37–R43 and R49–R52 are exclusive to *H. valentinum* and not shared with any  
676 other taxon (Fig. 2A; Electr. Suppl.: Fig. S3), but they are closely related to ribotypes detected in *H.*

677 *stoechas* specimens from the Iberian Peninsula (Fig. 2B; Electr. Suppl.: Fig. S3). These results indicate  
678 that *H. valentinum* was most likely derived from multiple ancient hybridization events, with *H. pendulum*  
679 and *H. stoechas* as parental species, as also suggested in a previous study (Galbany-Casals & al., 2006a)  
680 and morphological data presented here (Fig. 6; Electr. Suppl.: Fig. S4). Although one of the detected  
681 haplotypes in *H. valentinum*, H1, is also the most common haplotype in *H. pendulum*, the presence of an  
682 exclusive haplotype (H7) and the previously listed exclusive ribotypes indicate a certain current isolation  
683 of *H. valentinum* from the parental taxa.

684 The existence of current hybridization within the *H. pendulum* complex or between its members  
685 and other taxa of sect. *Stoechadina* was not an aim of the present study, and thus was not explicitly  
686 addressed. However, it should be noted that lineages of recent hybrid origin could also be prone to  
687 contemporary hybridization, as they can maintain gene flow with their parental taxa when no effective  
688 and strong reproductive barriers exist between them (Smitsen & al., 2007; Conesa & al., 2010). Current  
689 hybridization between the different species of the *H. pendulum* complex as accepted here is most  
690 probably rare given that they are not sympatric at present. However, current interspecific hybridization  
691 could be occurring in at least three cases involving a member of the *H. pendulum* complex and other  
692 members of sect. *Stoechadina*. One is *H. saxatile* that coexists with *H. italicum* in Sardinia; the second is  
693 *H. valentinum* which currently seems to hybridize with *H. stoechas* in coastal populations where both  
694 species coexist; and the third is *H. pendulum* that is sympatric with *H. crassifolium* in Majorca. In these  
695 three cases, occasional intermediate specimens have been detected in the vicinity, only separated by a few  
696 meters, of each pair of species involved (M. Galbany-Casals & L. Sáez, pers. obs.). There are several  
697 factors that support the hypothesis of a hybrid origin of the morphological intermediate specimens: (1) the  
698 coexistence of both parental species and the intermediate specimens in the same location (M. Galbany-  
699 Casals & L. Sáez, pers. obs.); (2) the partial overlap in flowering time of the *Helichrysum* species  
700 involved (Galbany-Casals & al., 2006a); (3) the low specificity of pollinator species observed in  
701 *Helichrysum* that may favour ongoing genetic exchange among species (Gil, 1994); and (4) the apparent  
702 lack of postzygotic barriers after interspecific gene flow (Conesa & al., 2012). Conesa & al. (2012)  
703 studied in detail the morphological and genetic variation of *H. pendulum* and *H. crassifolium* in the  
704 Balearic Islands and concluded that the patterns observed—the existence of a continuous and overlapping  
705 range in the leaf features that discriminate the two species, and the presence of intragenomic ETS  
706 polymorphisms in both species—were mainly caused by ongoing hybridization between them, and  
707 possibly with other species as well. In the present study, we have also detected intraspecific ribotype  
708 polymorphism within genomes affecting most of the species, where the ribotypes of a given specimen are  
709 not closest relative to each other in the nuclear gene tree (Electr. Suppl.: Table S1, Fig. S2). This  
710 phenomenon may be evidence of relatively recent interspecific hybridization, as revealed by the shared  
711 ribotypes among different species within the complex. However, we found no shared ribotypes between  
712 species from the *H. pendulum* complex and other species of sect. *Stoechadina* (Fig. 2; Electr. Suppl.:  
713 Table S1, Figs. S2, S3). This could be because the occasional intermediate specimens that could have  
714 originated from current hybridization were not included in the study, but also because of the intrinsic  
715 limitations of the software Phase, that only retrieves a maximum of two alleles in each individual. This  
716 potentially could underestimate the amount of variation found in the ribosomal DNA.

717  
718 **Revised taxonomic treatment of the *Helichrysum pendulum* complex.** — The present  
719 study sheds light on the delimitation of taxa of the *H. pendulum* complex. It differs from all previous  
720 taxonomic treatments in three remarkable aspects: (1) it includes a complete study of numerous  
721 specimens from all taxa of the complex, including representatives from the entire distribution area; (2)  
722 both morphological and molecular data are provided and analysed in detail; and (3) members of the *H.*  
723 *pendulum* complex are studied together with representatives of all other members of sect. *Stoechadina*.  
724 This comprehensive approach contributes not only to the characterization of the taxa of the *H. pendulum*  
725 complex but also to the interpretation of the evolutionary events underlying their origin.

726 In the present study, a species is defined in an attempt to fulfil two main criteria: (1) it must be  
727 constituted by a population or a group of populations that are morphologically recognizable by a set of  
728 common quantitative and/or qualitative traits, simultaneously permitting its differentiation from related  
729 species; and (2) its members should have a common origin—including a hybrid origin—and thus be

730 genetically closely related to one another and genetically distinguishable from other species. However, it  
731 is important to state that these two ideal criteria are difficult to meet in groups with two characteristics, as  
732 observed in the *H. pendulum* complex: (1) the group is composed of very closely related taxa, in which  
733 morphological variation is sometimes subtle and gradual between taxa; and (2) shows past and present  
734 hybridization between species. For these reasons, additional data on the ecology and geographic  
735 distribution of the studied populations, gathered over many years of observation of wild populations,  
736 provide valuable information for the finally adopted taxonomic treatment.

737 The proposed taxonomical framework presented here solves a long-standing problem of species  
738 identification in the *H. pendulum* complex. With our present proposal, the accuracy of correct assignment  
739 of a specimen to one of the five retained species in the *H. pendulum* complex is about 98% using  
740 morphological characters. We provide the characters identified as taxonomically relevant and useful to  
741 separate the different taxa recognized here, although a certain overlap of the quantitative features of the  
742 data was revealed by the multivariate analyses. The taxonomically valuable characters include the  
743 morphology of vegetative traits—eglandular indumentum of the adaxial side of leaves, glandular  
744 indumentum of the abaxial side of leaves, and the presence of succulent leaves—and reproductive traits—  
745 number of capitula per synflorescence, number of pistillate and hermaphroditic florets per capitulum,  
746 outermost involucre bract length, width, texture, and eglandular indumentum, and innermost involucre  
747 bract width and number of involucre bracts per capitulum. According to these morphological characters  
748 and the evidence from molecular data, we recognize five species within the complex: *H. pendulum*, *H.*  
749 *errerae*, *H. melitense*, *H. valentinum* and *H. saxatile*. The degree of differentiation in terms of  
750 morphology and molecular data is not equivalent for all them. The first three species are clearly  
751 recognizable by qualitative and quantitative morphological traits in multivariate analyses and ANOVAs  
752 (Fig. 4; Electr. Suppl.: Table S2, Fig. S5), and additionally they are genetically distinguishable from the  
753 rest by nrDNA, cpDNA or both molecular markers (Figs. 1, 2; Electr. Suppl.: Table S1, Figs. S2, S3).  
754 *Helichrysum valentinum* and *H. saxatile* are reported here to have a putative ancient hybrid origin, with  
755 *H. pendulum* as one of the parental species involved, and *H. stoechas* and *H. italicum* as the second  
756 parental species involved, respectively. Their hybrid origin probably determines that these two species are  
757 only distinguishable by quantitative characters from their parental species, and that a notable degree of  
758 overlapping with one or both of them exists (Figs. 4, 5). In these two cases, molecular information  
759 provides the clue that points to their recognition at the species level, given that it provides evidence of: (1)  
760 their past hybrid origin, (2) the particular species involved in their origin, and (3) their current isolation,  
761 evidenced by their genetic differentiation, i.e. the possession of private nrDNA and cpDNA markers.  
762 Hereafter, we provide detailed discussion for each case.

763 *Helichrysum pendulum* in a strict sense is suggested herein to represent a single polymorphic  
764 taxon, which is consistent with Galbany-Casals & al. (2006a; as *H. rupestre* DC.). Considering  
765 nomenclatural priority (Aghababayan & al., 2007) and the results obtained, the name *H. pendulum*, based  
766 on plants from the Madonie Mountains in Sicily, should be applied to populations of the *H. pendulum*  
767 complex distributed throughout the Balearic Islands, Gibraltar, Morocco, Algeria, Sicily and the  
768 Marettimo islet. This species contains several local genetic particularities, mainly in northern Africa,  
769 Gibraltar and Sicily (Figs. 1B, 2A). However, these slightly divergent populations could not be  
770 distinguished by morphometric data, suggesting that they reflect the phylogeographical history of the  
771 species but do not merit taxonomic recognition.

772 Several investigations have been performed in Sicily to resolve relationships among *Helichrysum*  
773 entities and to clarify their systematics (Pignatti, 1982; Giardina & al., 2007; Scialabba & al., 2008). The  
774 lack of an assessment of the Sicilian populations in the context of the variation of the entire *H. pendulum*  
775 complex led these studies to report numerous taxa at the infraspecific and/or species level. Here, we  
776 evaluated the variation in the whole distribution area of the species complex and increased the number of  
777 individuals sampled in comparison to previous work. Our combined results for the molecular and  
778 morphological data reflect the inconsistency of distinctive traits that makes the differentiation of most of  
779 the previously recognized entities very difficult. Only the populations from mountains of western Sicily  
780 (Madonie Mountains) and southern Sicily deserve special attention. Some populations from the Madonie  
781 Mountains have been considered a separate taxon restricted to that area and named *H. pendulum* in the  
782 treatments proposed by Presl (1826), Gussone (1844), Lojacono Pojero (1889–1908), Greuter (2006+)

783 and Scialabba & al. (2008), independent from other populations from the Madonie Mountains, named *H.*  
784 *nebrodense*, and from populations from the western coastal part of the island, which have been considered  
785 as *H. panormitanum*. Scialabba & al. (2008), using AFLP markers, argued that *H. pendulum* populations  
786 were genetically isolated and distant from other Sicilian locations. In the present study, *H. pendulum*  
787 shares haplotype H2 with other mountain populations from Sicily belonging to *H. panormitanum* and *H.*  
788 *nebrodense*, but has an almost exclusive ribotype (R62), only shared with *H. saxatile* but not present in  
789 other Sicilian populations (Figs. 1, 2). *Helichrysum nebrodense* has an exclusive ribotype (R58) but also  
790 shares ribotype R56 with other Sicilian populations. Given the low level of genetic differentiation of *H.*  
791 *pendulum*, *H. panormitanum* and *H. nebrodense*, and the lack of morphological characters to distinguish  
792 them, we consider all of them to belong to a single species, *H. pendulum*. The taxonomic status of the  
793 populations from southern Sicily, traditionally assigned to *H. hyblaeum*, remains unclear. In this case, we  
794 detected genetic singularities, such as the exclusive haplotypes (H3 and H4) and ribotypes (R3, R4, R5,  
795 R6 and R70). Scialabba & al. (2008) found that *H. hyblaeum* was genetically isolated from the other  
796 Sicilian populations. However, this genetically structured pattern of variation is barely reflected in the  
797 morphology to allow the differentiation of these populations. Thus, we tentatively do not consider that  
798 such southern Sicilian populations deserve taxonomic recognition, although more detailed studies focused  
799 on these populations are desirable. In fact, ribotypes detected in *H. hyblaeum* are closely related to  
800 specimens of *H. stoechas* from Tunisia and Greece (Fig. 2B, Electr. Suppl.: Fig. S3). These results are  
801 consistent with previous suggestions concerning possible hybridization between *H. hyblaeum* and *H.*  
802 *stoechas* in southern Sicily (Galbany-Casals & al., 2006a), or a possible hybrid origin of the former.

803 The results of the DNA analyses showed that *H. fontanesii* populations (Cambessèdes, 1827;  
804 Greuter, 2006+) from the Balearic Islands, Morocco and Algeria are poorly differentiated genetically.  
805 Moreover, the absence of marked distinctive morphological characteristics (Fig. 4A) led us to include this  
806 taxon within the variable *H. pendulum*. Its separation was originally based on the subglabrous to  
807 arachnoid leaves on the adaxial surface, but this is not true for all specimens from the area inhabited by *H.*  
808 *fontanesii*, and this feature can also be seen in some Sicilian specimens. *Helichrysum boissieri*, which has  
809 been described from Gibraltar (Nyman, 1879; Greuter, 2006+), showed genetic differentiation in both  
810 markers (Figs. 1B, 2A), but again it could not be morphologically recognized as a distinct species. It is  
811 noteworthy that neither *H. fontanesii* nor *H. boissieri* have been recognized in recent local floras, and  
812 instead both are treated as *H. rupestre*, a broadly distributed taxon that also includes the Sicilian  
813 populations (Valdés & al., 1987; Boldòs & Vigo, 1996). Fennane & Ibn Tattou (1998) indicated that *H.*  
814 *boissieri* is also present in northern Morocco, but that particular population is composed of *H. stoechas*  
815 specimens (Galbany-Casals, pers. obs.).

816 *Helichrysum errerae* is supported here as a distinct species restricted to Pantelleria Island and  
817 clearly characterized by completely or partially herbaceous outermost involucre bracts that are covered  
818 with a dense eglandular indumentum (Fig. 4, Electr. Suppl.: Table S2). These qualitative differences with  
819 respect to *H. pendulum* justify its recognition at the species level even in the most synthetic treatments  
820 (Galbany-Casals & al., 2006a). It has also been reported to be distributed in Marettimo islet, with a  
821 different variety, *H. errerae* var. *messerii*, based on genetic similarities of populations from the two  
822 islands detected using AFLPs (Scialabba & al., 2008). However, here we show that specimens from  
823 Marettimo islet are morphologically indistinguishable from *H. pendulum*, which in turn is clearly  
824 separated from *H. errerae* (Fig. 4). Genetically, Pantelleria populations contain two exclusive ribotypes  
825 (R68 and R69; Fig. 2) which are closely related to ribotype R72 found in Marettimo islet, in agreement  
826 with the findings of Scialabba & al. (2008), but are also related to ribotype R70 found in *H. pendulum*.

827 Another case of island endemism is *H. melitense* from Gozo Island (Malta). Maltese populations  
828 are recognized here as a separate species based on their distinct morphology (Figs. 4, 6) and the high level  
829 of genetic differentiation seen in their private haplotype (H15; Fig. 1) and ribotypes (R1 and R2; Fig. 2).  
830 These are noticeably different from any other haplotypes and ribotypes in the section. Its taxonomic status  
831 has been historically controversial. This taxon was originally described as a variety of *H. pendulum* (sub  
832 *H. rupestre*) by Pignatti (1980) and later recognized at the species level by Brullo & al. (1988) only  
833 based on its wider leaves relative to those of *H. pendulum* in Sicily. Later, Galbany-Casals & al. (2006a)  
834 considered *H. melitense* a synonym for *H. rupestre*, arguing that leaf width is very variable within  
835 *Helichrysum* species, although minimal material was studied. Here, a more complete morphometric study



836 revealed that *H. melitense* leaves are significantly wider than those in other taxa of the complex and  
837 noticeably succulent (Electr. Suppl.: Table S2), a trait that was not noticed in previous work based on the  
838 study of old herbarium material. Both morphological and molecular data confirm the particularities of the  
839 Maltese populations and therefore support the recognition of *H. melitense*.

840 *Helichrysum valentinum* has been treated as an independent species (Rouy, 1888), as a subspecies  
841 of *H. pendulum* under different names (Mateo, 2005; Mateo & Crespo, 2008; Crespo & Mateo, 2010) or  
842 as a synonym of *H. pendulum* (sub *H. rupestre*; Bolòs & Vigo, 1996). As discussed above, it was  
843 considered to be of hybrid origin between *H. rupestre* and *H. stoechas* by Galbany-Casals & al. (2006a),  
844 based on the observed intermediate morphological characters between its putative parents. These  
845 observations are supported here by molecular data, as discussed above, and by morphological analyses  
846 (Fig. 5A, Electr. Suppl.: Fig. S4). The hybrid origin strongly supports its recognition as a species instead  
847 of as a subspecies of any of the parental taxa. *Helichrysum valentinum* is distinct in terms of having fewer  
848 capitula per synflorescence than *H. pendulum* (Electr. Suppl.: Table S2), in accordance with the  
849 observations of Mateo (2005). Additionally, we found that *H. valentinum* has shorter leaves compared to  
850 the remaining species in the complex (Fig. 6; Electr. Suppl.: Table S2), which are not necessarily  
851 narrower as suggested by Mateo (2005). Galbany-Casals & al. (2006a) reported that several intermediate  
852 specimens can be observed between *H. valentinum* and *H. stoechas* in coastal localities where the two  
853 species coexist, which, as discussed above, could be of recent hybrid origin between the two species.

854 The populations from central-eastern Sardinia also deserve special attention. These populations  
855 were originally described as a separate species that is endemic to Sardinia, *H. saxatile* (Moris,  
856 1840–1843), as recognized by Clapham (1976), Pignatti (1982), and Baccheta & al. (2003), mainly based  
857 on smaller and narrower capitula and leaves than in *H. pendulum* (sub *H. rupestre*). Later, Galbany-Casals  
858 & al. (2006a) considered it synonymous with *H. rupestre*, given that no qualitative characters allowed the  
859 separation of the two taxa. Here, we support the taxonomic recognition of *H. saxatile*, despite a certain  
860 overlap with the morphological variation of *H. pendulum* in the PCA and CDA analyses (Figs. 4, 5B;  
861 Electr. Suppl.: Fig. S4). As suggested in previous investigations, capitula are significantly shorter in  
862 *H. saxatile* (Electr. Suppl.: Table S2), and we further discovered a smaller total number of florets per  
863 capitulum and shorter outermost involucre bracts (Electr. Suppl.: Table S2). Moreover, the high genetic  
864 diversity of Sardinian populations and their genetic differentiation from other populations of the  
865 *H. pendulum* complex is noteworthy, with three exclusive haplotypes (H12, H13 and H14; Fig. 1B) and eight  
866 exclusive ribotypes (R60, R61, R63, R64, R65, R66, R67 and R71; Fig. 2). This genetic differentiation  
867 from other taxa is due, in part and as discussed above, to *H. italicum*, one of the putative parental taxa  
868 involved in its origin. Our morphological analysis (Fig. 5B) supports the hypothesis of a hybrid origin  
869 since it revealed a morphological gradient in the Sardinian populations, with varying degrees of similarity  
870 to the putative parental species; the appearance of some specimens is similar to *H. pendulum*, while others  
871 have smaller and narrower capitula like *H. italicum*. In general, *H. saxatile* is morphologically much more  
872 similar to *H. pendulum* than to *H. italicum*. However, as in the case of *H. valentinum*, its hybrid origin  
873 strongly supports its recognition as an independent species, and it should not be subordinated at any  
874 infraspecific rank under one of its parental species. *Helichrysum pendulum* does not currently exist in  
875 Sardinia, in contrast to *H. italicum*. Current gene flow between *H. saxatile* and *H. italicum* could be still  
876 occurring, as suggested by the presence of individuals with intermediate morphological features between  
877 these two species in localities where they coexist (Galbany-Casals & al., 2006a; M. Galbany-Casals and  
878 L. Sáez, pers. obs.).

## 881 ■ TAXONOMIC TREATMENT

882  
883 Based on the discussion above, the following taxonomic treatment with a standard identification  
884 key is presented. Given the hybrid origin of *H. saxatile* and *H. valentinum*, some morphological overlap  
885 may exist between each of them and *H. pendulum*. We also provide the habitat requirements and the  
886 distribution range for each taxon, and a complete nomenclatural treatment.

888 **Key to the species of the *Helichrysum pendulum* complex**

889

890 1. Outermost involucre bracts (0.5)1–1.8(2) mm wide, totally or partially herbaceous, densely tomentose  
891 ..... *H. errerae*

892

893 1. Outermost involucre bracts (0.8)1.5–3.2 mm wide, totally papery, glabrous to subglabrous ..... 2

894

895 2. Leaves succulent, densely tomentose on both sides; basal and median cauline leaves of flowering and  
896 vegetative stems (1.8)2.7–4.7(5.8) mm wide. Capitula 5.7–8 mm long ..... *H. melitense*

897

898 2. Leaves not succulent, subglabrous to densely tomentose on the adaxial side, densely tomentose on the  
899 abaxial side; basal and median cauline leaves of flowering and vegetative stems (0.6)1–4(7) mm wide.

900 Capitula (4)5–7(8) mm long ..... 3

901

902 3. Basal and median cauline leaves of flowering and vegetative stems (8.5)12–36(53) mm long,  
903 densely tomentose and sparsely to densely glandular on the abaxial side, rarely eglandular.

904 Synflorescences with (5)9–30(53) capitula ..... *H. valentinum*

905

906 3. Basal and median cauline leaves of flowering and vegetative stems 10–70(85) mm long, densely  
907 tomentose and eglandular to sparsely glandular on the abaxial side. Synflorescences with

908 (7)12–100(146) capitula ..... 4

909

910 4. Leaves arachnoid-tomentose to densely tomentose on the adaxial side. Capitula 4.5–6.5(7) mm  
911 long, with (20)24–47 florets, 4–13 pistillate and 13–37 hermaphroditic. Outermost involucre bracts

912 1.9–3(3.2) mm long ..... *H. saxatile*

913

914 4. Leaves subglabrous to arachnoid, rarely arachnoid-tomentose or tomentose, on the adaxial side.  
915 Capitula (4)5–7(8) mm long, with (23)30–74(88) florets, (5)7–24(29) pistillate and (21)25–55(62)

916 hermaphroditic. Outermost involucre bracts 2–4.9 mm long ..... *H. pendulum*

917

918

919 ***Helichrysum errerae*** Tineo, Pl. Rar. Sicil. 2: 27. 1846 ≡ *H. saxatile* subsp. *errerae* (Tineo) Nyman,

920 Consp. Fl. Eur.: 381. 1879 ≡ *H. saxatile* var. *errerae* (Tineo) Fiori in Fiori & Paol., Fl. Italia 3:

921 282. 1904 ≡ *H. saxatile* var. *errerae* (Tineo) Zangh., Flora Italica 1: 695. 1976, *comb. superfl.* ≡

922 *H. rupestre* var. *errerae* (Tineo) Pignatti in Giorn. Bot. Ital. 113 (5–6): 363. 1980 – Lectotype

923 (designated by Aghababayan & al., 2007: 1286, superseding the neotype proposed by Galbany-

924 Casals & al., 2006c: 494): “*Helichrysum Errerae* Tin., Pantelleria” [manu Tineo], herb. siculum

925 Gussonei (NAP).

926

927 *Habitat.* – Maritime volcanic rocks and cliffs. Altitudinal range: 10–118 m.

928 *Distribution.* – Endemic to Pantelleria Island (SW Sicily).

929

930 ***Helichrysum melitense*** (Pignatti) Brullo, Lanfranco, Pavone & Ronsisvalle in Giorn. Bot. Ital. 122,

931 suppl. 1: 9. 1988 ≡ *H. rupestre* var. *melitense* Pignatti in Giorn. Bot. Ital. 113 (5–6): 363. 1980 –

932 Holotype: Insula Gaulos, Cala Dueira, in rupibus maritimus, 22–IV–1874, *Duthie s.n.* (FI

933 001872!).

934

935 *Habitat.* – Intact limestone coastal cliffs and scree, preferring full sun. Occasionally found along the  
936 plateau on top of the cliffs. Altitudinal range: 15–100 m.

937 *Distribution.* – Endemic to western cliffs of the island of Gozo and Fungus Rock (Malta).

938

939 ***Helichrysum pendulum*** (C.Presl) C.Presl, Fl. Sicul.: xxix. 1826 ≡ *Gnaphalium pendulum* C.Presl in

940 J.Presl & C.Presl, Delic. Prag.: 97. 1822 ≡ *H. rupestre* subsp. *pendulum* (C.Presl) Arcang., Comp.

941 Fl. Ital.: 376. 1882 ≡ *H. rupestre* var. *pendulum* (C.Presl) Fiori, Nuov. Fl. Italia 2: 890. 1928,

942 *comb. superfl.* – Lectotype (designated by Aghababayan & al., 2007: 1286): “*Helichrysum*

943 *pendulum* Pr., *Gnaphalium pendulum* Pr. del. *Pendulum* in praeruptis mont. Scalune Nebrodum. h

944 Jul. 1817” (PR 616046 photo!).

945

- 946 = *Gnaphalium rupestre* Raf., Précis Découv. Somiol.: 41. 1814, *nom. illeg.* (non. Pourr. in Hist. & Mém.  
947 Acad. Roy. Sci. Toulouse 3: 320. 1788) ≡ *Helichrysum rupestre* DC., Prodr. 6: 182. 1838, *nom.*  
948 *illeg.* ≡ *H. stoechas* subsp. *rupestre* (Raf.) Maire in Jahand. & Maire, Cat. Pl. Maroc 3: 751. 1934  
949 – Neotype (designated by Galbany-Casals & al., 2006c: 492): Palermo, in rupibus calcareis, V,  
950 *Todaro 551* (PAL 8720!; isoneotypes: FI 001852!, FI 001853!, K 001273168!, P!, PH 1029697  
951 photo!).  
952  
953 = *Helichrysum fontanesii* Cambess. in Mém. Mus. Hist. Nat. 14: 270. 1827 ≡ *H. rupestre* var. *fontanesii*  
954 (Cambess.) DC., Prodr. 6: 182. 1838 ≡ *H. stoechas* f. *fontanesii* (Cambess.) Knoche, Fl. Balear. 2:  
955 459. 1922 ≡ *H. rupestre* var. *fontanesii* (Cambess.) Magallon, Fl. Veg. Alicante: 356. 1972, *comb.*  
956 *superfl.* ≡ *H. pendulum* subsp. *fontanesii* (Cambess.) M.B.Crespo & Mateo in Flora Montiber. 45:  
957 92. 2010 – Lectotype (designated by Rosselló & Sáez, 2000: 32): Lluch, 20–IV–1825,  
958 *Cambessèdes s.n.* (MPU-KNOCHE MPU 310728!; isolectotype: P!).  
959  
960 = *Helichrysum nebrodense* Heldr. in Ann. Accad. Aspir. Naturalisti 1: 286. 1843 ≡ *H. rupestre* subsp.  
961 *nebrodense* (Heldr.) Arcang., Comp. Fl. Ital.: 376. 1882 ≡ *H. rupestre* var. *nebrodense* (Heldr.)  
962 Fiori, Nuov. Fl. Italia 2: 672. 1927, *comb. superfl.* – Lectotype (designated by Aghababayan & al.,  
963 2007: 1286, superseding the neotype proposed by Galbany-Casals & al., 2006c: 496):  
964 “*Helichrysum nebrodense?* Nob. inedit., in rupibus calcareis prope Isnello, 12 Jun. 1840. *Theod. de*  
965 *Heldreich*” [manu Heldreich], herb. siculum Gussonei (NAP).  
966  
967 = *Helichrysum panormitanum* Tineo ex Guss., Fl. Sicul. Syn. 2: 467. 1844 ≡ *H. panormitanum* var.  
968 *angustifolium* Tineo ex Guss., Fl. Sicul. Syn. 2: 467. 1844, *nom. illeg.* ≡ *Gnaphalium*  
969 *panormitanum* (Tineo ex Guss.) Bertol., Fl. Ital. 9: 135. 1853 ≡ *H. rupestre* subsp. *panormitanum*  
970 (Tineo ex Guss.) Arcang., Comp. Fl. Ital.: 375. 1882 – Lectotype (designated by Aghababayan &  
971 al., 2007: 1286): In rupibus calcareis prope Panormum, scala di Maseddu [manu Tineo], “*Tineo*”  
972 [manu Gussone], herb. Siculum Gussonei (NAP photo!; isotype: FI 001854!).  
973  
974 = *Helichrysum panormitanum* var. *latifolium* Guss., Fl. Sicul. Syn. 2: 467. 1844 – Lectotype (designated  
975 by Galbany-Casals & al., 2006c: 497, amended by Aghababayan & al., 2007: 1287): “*Elichrysum*  
976 *panormitanum* Tin. b. *latifolium* Guss.!! [scripsit] Grande, 1916”; “Maggio, Bagheria a Capo  
977 Zafferano” [manu Gussone], [Gussone], herb. siculum Gussonei (NAP photo!).  
978  
979 = *Helichrysum pendulum* var. *compactum* Guss., Fl. Sicul. Syn. 2: 467. 1844 – Lectotype (designated by  
980 Aghababayan & al., 2007: 1287): specimen bearing two labels: “Luglio, Madonie”, and “6b.  
981 *Helichrysum pendulum* b. *compactum* Supl. syn. 2 p. 467, Junio, Julio h, in rupibus calcareis  
982 montosis.” [manu Gussone], herb. siculum Gussonei (NAP).  
983  
984 = *Helichrysum pendulum* var. *laxiusculum* Guss., Fl. Sicul. Syn. 2: 467. 1844 – *Ind. loc.*: “Busambra  
985 (Tin.), Monte de Cani, Caltavuturo, Vicari, Pizzuta = et in Marettimo”. = *Helichrysum stramineum*  
986 Guss., Fl. Sicul. Syn. 2: 467. 1844 ≡ *H. rupestre* var. *stramineum* (Guss.) Fiori, Nuov. Fl. Italia 2:  
987 672. 1927 – Lectotype (designated by Galbany-Casals & al., 2006a: 499): Sferracavallo, *Tineo*,  
988 [herb. siculum Gussonei] (NAP photo!).  
989  
990 = *Helichrysum boissieri* Nyman, Consp. Fl. Eur. 1: 381. 1879 ≡ *H. rupestre* var. *boissieri* (Nyman)  
991 Willk., Suppl. Prodr. Fl. Hispan.: 79. 1893 ≡ *H. stoechas* subsp. *boissieri* (Nyman) Maire in  
992 Jahand. & Maire, Cat. Pl. Maroc. 3: 751. 1934 – Lectotype (designated by Galbany-Casals & al.,  
993 2006c: 494): Gibraltar, in rupibus, V–1837, *Boissier s.n.* (G 00446427!; isolectotypes: G  
994 00446428!; G-DC G 00470401!, K 001273166!, P!, W 0045868!).  
995  
996 = *Helichrysum porcarii* Tineo ex Lojac. in Natural. Sicil. 2: 182. 1883 – Lectotype (designated by  
997 Aghababayan & al., 2007: 1287): “*Helichrysum porcari* Tin., Agosto, Madonie, Salto della Botte,  
998 *Porcari*” [manu Porcari], herb. siculum Gussonei (NAP).  
999  
1000 = *Helichrysum wickstromii* Tineo ex Lojac. in Natural. Sicil. 2: 182. 1883 – Lectotype (designated by  
1001 Aghababayan & al., 2007: 1287): “Giugno 49, *Elichrysum Wickströmii* Tin. inedit., Pizzuta” [manu  
1002 Tineo], herb. siculum Gussonei (NAP).  
1003

- 1004 = *Helichrysum fontanesii* var. *latifolium* Font Quer in Bol. Soc. Esp. Hist. Nat. 20: 148. 1920 ≡ *H.*  
1005 *rupestre* f. *latifolium* (Font Quer) O.Bolòs & Vigo in Collect. Bot. (Barcelona) 14: 103. 1983 –  
1006 Lectotype (designated by Rosselló & Sáez, 2000: 32): Eivissa, Cala de les Torretes, pr. Sta. Agnès,  
1007 29–V–1918, *Gros s.n.* (BC 30830!).  
1008  
1009 = *Helichrysum rupestre* var. *messerii* Pignatti in Giorn. Bot. Ital., 113 (5–6): 363. 1980 ≡ *H. errerae* var.  
1010 *messerii* (Pignatti) Raimondo in Bocconeia 20: 11. 2007 – Holotype: Marettimo, in rupibus  
1011 calcareis maritimis, VI–VIII–1900, Ross 243 (Ross Herb. Sic. 243, Sub. *Helichrysum rupestre* var.  
1012 *pendulum*) (FI 001873!; isotypes: G 00418267!, K 001273169!, P!).  
1013  
1014 = *Helichrysum hyblaenum* Brullo in Colloq. Phytosociol. 21: 630. 1995 – Holotype: Valle del f. Irminio,  
1015 fra Modica e Ragusa, 4–V–1983, *Brullo s.n.* (CAT 005229; isotypes: FI 001863!, FI 001864!, FI  
1016 001865!).  
1017  
1018 *Habitat.* – Limestone rock crevices and maritime cliffs. Altitudinal range: 15–1850 m.  
1019 *Distribution.* – Western-central Mediterranean area: S Iberian Peninsula (Gibraltar) and Balearic Islands  
1020 (Majorca, Ibiza, Cabrera and Es Vedrà and Vedranell islets), Morocco, Algeria, Sicily and Marettimo islet.  
1021  
1022 *Helichrysum saxatile* Moris, Fl. Sardoia 2: 387, t. 82. 1840–1843 ≡ *Gnaphalium saxatile* (Moris) Bertol.,  
1023 Fl. Ital. 9: 136. 1853, *nom. illeg.* (non L., Sp. Pl.: 857. 1753) – Lectotype (designated by Arrigoni  
1024 & al., 1980: 245): Baunei ad rupes, *s.d.*, *Moris s.n.* (SASSA photo!).  
1025  
1026 *Habitat.* – Limestone rock crevices, rocky slopes and cliffs. Altitudinal range: 317–1000 m.  
1027 *Distribution.* – Endemic to Sardinia.  
1028  
1029 *Helichrysum valentinum* Rouy in T. Durand & B.D. Jackson, Index Kew., Suppl. 1: 199. 1902 – Neotype  
1030 (designated by Galbany-Casals & al., 2006c: 499): Denia, Le Mongo ça et là sur les parois des  
1031 hauts rochers, 1–VI–1889, *Rouy s.n.* (LY 0006931 photo!).  
1032  
1033 *Habitat.* – Limestone rock crevices, in mountain areas and coastal cliffs. Altitudinal range: 30–1300 m.  
1034 *Distribution.* – E of the Iberian Peninsula in Alicante province.  
1035  
1036

## 1037 ■ ACKNOWLEDGMENTS

1038  
1039 We are grateful to the curators of all herbaria and to J.J. Aldasoro, S. Arrabal, E. Blanco, J.A.  
1040 Devesa, N. Garcia-Jacas, A. Hilpold, S. Massó, S. Lanfranco, J.X. Soler, A. Susanna, and J. Xiberras for  
1041 providing plant material or field assistance for this work. J.X. Soler and J. Xiberras have also provided  
1042 helpful information and stimulating discussion on *H. valentinum* and *H. melitense*, respectively. Three  
1043 anonymous reviewers and the editors made valuable suggestions that contributed to improve this work.  
1044 Financial support from the Spanish Ministerio de Ciencia e Innovación CGL2007–60781/BOS,  
1045 CGL2009–13322–C03–03/BOS, CGL2010–18631/BOS) and the Catalan government ('Ajuts a grups  
1046 consolidats' 2009/SGR/00439 and 2014/SGR/514) is also acknowledged.  
1047  
1048

## 1049 ■ LITERATURE CITED

- 1050  
1051 Aghababyan, M., Greuter, W., Mazzola, P. & Raimondo, F.M. 2007. Typification of Sicilian  
1052 *Helichrysum* (Compositae) revisited. *Taxon* 56: 1285–1288. <http://dx.doi.org/10.2307/25065922>  
1053 Arrigoni, P.A., Camarda, I., Corrias, B., Diana-Corrias, S., Raffaelli, M. & Valsecchi, F. 1980. Le  
1054 piante endemiche della Sardegna. *Boll. Soc. Sarda. Sci. Nat.* 19: 217–254.  
1055 Arroyo, J., Aparicio, A., Albaladejo, R.G., Muñoz, J. & Braza, R. 2008. Genetic structure and  
1056 population differentiation of the Mediterranean pioneer spiny broom *Calicotome villosa* across  
1057 the Strait of Gibraltar. *Biol. J. Linn. Soc.* 93: 39–51. [http://dx.doi.org/10.1111/j.1095-](http://dx.doi.org/10.1111/j.1095-8312.2007.00916.x)  
1058 [8312.2007.00916.x](http://dx.doi.org/10.1111/j.1095-8312.2007.00916.x)  
1059 Bacchetta, G., Brullo, S. & Mossa, L. 2003. Note tassonomiche sul genere *Helichrysum* Miller  
1060 (Asteraceae) in Sardegna. *Inf. Bot. Ital.* 35: 217–225.

- 1061 **Baldwin, B.G. & Markos, S.** 1998. Phylogenetic utility of the external transcribed spacer (ETS) of 18S–  
1062 26S rDNA: congruence of ETS and ITS trees of *Calycadenia* (Compositae). *Molec. Phylogenet.*  
1063 *Evol.* 10: 449–463. <http://dx.doi.org/10.1006/mpev.1998.0545>
- 1064 **Barres, L., Vilatersana, R., Molero, J., Susanna, A. & Galbany-Casals, M.** 2011. Molecular  
1065 phylogeny of *Euphorbia* subg. *Esula* sect. *Aphyllis* (Euphorbiaceae) inferred from nrDNA and  
1066 cpDNA markers with biogeographic insights. *Taxon* 60: 705–720.
- 1067 **Beerli, P., Hotz, H. & Uzzell, T.** 1996. Geologically dated sea barriers calibrate a protein clock for  
1068 Aegean water frogs. *Evolution* 50: 1676–1687. <http://dx.doi.org/10.2307/2410903>
- 1069 **Blanco-Pastor, J.L., Vargas, P & Pfeil, B.E.** 2012. Coalescent simulations reveal hybridization and  
1070 incomplete lineage sorting in Mediterranean *Linaria*. *PLoS ONE* 7: e39089.  
1071 <http://dx.doi.org/10.1371/journal.pone.0039089>
- 1072 **Bolòs, O. & Vigo, J.** 1996. *Flora dels Països Catalans*, vol. 3. Barcelona: Ed. Barcino.
- 1073 **Brullo, S., Lanfranco, E., Pavone, P. & Ronsisvalle, G.** 1988. Taxonomical notes on the endemic flora  
1074 of Malta. *Giorn. Bot. Ital.* 122: 9.
- 1075 **Cambessèdes, J.** 1827. Enumeratio plantarum, quas in insulis Balearibus collegit J. Cambessèdes,  
1076 earumque circa Mare Mediterraneum distributio geographica. *Mém. Mus. Hist. Nat.* 14: 173–  
1077 335.
- 1078 **Clapham, A.R.** 1976. *Helichrysum* Mill. Pp. 128–131 in: Tutin, T.G., Heywood, V.H., Burges, N.A.,  
1079 Moore, D.M., Valentine, D.H., Walters, S.M. & Webb, D.A. (eds.), *Flora Europaea*, vol. 4.  
1080 Cambridge: Cambridge University Press.
- 1081 **Clement, M., Posada D. & Crandall K.A.** 2000. TCS: a computer program to estimate gene  
1082 genealogies. *Molec. Ecol.* 9: 1657–1659. <http://dx.doi.org/10.1046/j.1365-294x.2000.01020.x>
- 1083 **Comes, H.P. & Abbott, R.J.** 2001. Molecular phylogeography, reticulation, and lineage sorting in  
1084 Mediterranean *Senecio* sect. *Senecio* (Asteraceae). *Evolution* 55: 1943–1962.  
1085 <http://dx.doi.org/10.1111/j.0014-3820.2001.tb01312.x>
- 1086 **Conesa, M.A., Mus, M. & Roselló, J.A.** 2010. Who threatens who? Natural hybridization between  
1087 *Lotus dorycnium* and the island endemic *Lotus fulgurans* (Fabaceae). *Biol. J. Linn. Soc.* 101: 1–  
1088 12. <http://dx.doi.org/10.1111/j.1095-8312.2010.01456.x>
- 1089 **Conesa, M.A. Mus, M. & Roselló, J.A.** 2012. Leaf shape variation and taxonomic boundaries in two  
1090 sympatric rupicolous species of *Helichrysum* (Asteraceae: Gnaphalieae), assessed by linear  
1091 measurements and geometric morphometry. *Biol. J. Linn. Soc.* 106: 498–513.  
1092 <http://dx.doi.org/10.1111/j.1095-8312.2012.01889.x>
- 1093 **Corander, J., Sirén, J. & Arjas, E.** 2008. Bayesian spatial modelling of genetic population structure.  
1094 *Comput. Stat.* 23: 111–129. <http://dx.doi.org/10.1007/s00180-007-0072-x>
- 1095 **Corriveau, J.L. & Coleman, A.W.** 1988. Rapid screening method to detect potential biparental  
1096 inheritance of plastid DNA and results for over 200 angiosperm species. *Am. J. Bot.* 70: 1443–  
1097 1458. <http://dx.doi.org/10.2307/2444695>
- 1098 **Cowie, R.H. & Holland, B.S.** 2006. Dispersal is fundamental to biogeography and the evolution of  
1099 biodiversity on oceanic islands. *J. Biogeogr.* 33: 193–198. <http://dx.doi.org/10.1111/j.1365-2699.2005.01383.x>
- 1100 **Crespo, M.B. & Mateo, G.** 2010. Novedades taxonómicas y nomenclaturales para la Flora Valenciana,  
1101 II. *Fl. Montib.* 45: 89–102.
- 1102 **Cullings, K.W.** 1992. Design and testing of a plant-specific PCR primer from ecological and evolutionary  
1103 studies. *Molec. Ecol.* 1: 233–240. <http://dx.doi.org/10.1111/j.1365-294X.1992.tb00182.x>
- 1104 **Dayrat, B.** 2005. Towards integrative taxonomy. *Biol. J. Linn. Soc.* 85: 407–415.  
1105 <http://dx.doi.org/10.1111/j.1095-8312.2005.00503.x>
- 1106 **Doyle, J.J. & Dickson, E.E.** 1987. Preservation of plant samples for DNA restriction endonuclease  
1107 analysis. *Taxon* 36: 715–722. <http://dx.doi.org/10.2307/1221122>
- 1108 **Duggen, S., Hoernle, K., van den Bogaard, P., Rüpke, L. & Morgan, J.P.** 2003. Deep roots of the  
1109 Messinian salinity crisis. *Nature* 402: 602–606. <http://dx.doi.org/10.1038/nature01553>
- 1110 **Excoffier, L., Laval, G. & Schneider, S.** 2005. Arlequin (version 3.0): An integrated software package  
1111 for population genetics data analysis. *Evol. Bioinf. Online* 1: 47–50.
- 1112 **Excoffier, L., Smouse, P.E. & Quattro J.M.** 1992. Analysis of molecular variance inferred from metric  
1113 distances among DNA haplotypes: Application to human mitochondrial DNA restriction data.  
1114 *Genetics* 131: 479–491.
- 1115 **Fehrer, J., Gemeinholzer, B., Chrtek, J. & Bräutigam, S.** 2007. Incongruent plastid and nuclear DNA  
1116 phylogenies reveal ancient intergeneric hybridization in *Pilosella* hawkweeds (*Hieracium*,  
1117 Chichorieae, Asteraceae). *Molec. Phylogenet. Evol.* 42: 374–361.  
1118 <http://dx.doi.org/10.1016/j.ympev.2006.07.004>
- 1119

- 1120 **Felsenstein, J.** 1985. Confidence limits on phylogenies: An approach using the bootstrap. *Evolution* 39:  
1121 783–791. <http://dx.doi.org/10.2307/2408678>
- 1122 **Fennane, M. & Ibn Tattou, M.** 1998. Catalogue des plantes vasculaires rares, menacées ou -endémiques  
1123 du Maroc. *Bocconea* 8: 1–242.
- 1124 **Fernández-Mazuecos, M. & Vargas, P.** 2011. Historical isolation versus recent long-distance  
1125 connections between Europe and Africa in bifid toadflaxes (*Linaria* sect. *Versicolores*). *PLoS*  
1126 *ONE* 6: e22234. <http://dx.doi.org/10.1371/journal.pone.0022234>
- 1127 **Fiori, A.** 1927. *Nuova Flora Analitica d'Italia* 2. Firenze: Ed. M. Ricci.
- 1128 **Fiz, O., Valcárcel, V. & Vargas, P.** 2002. Phylogenetic position of Mediterranean Asteraceae and  
1129 character evolution of daisies (*Bellis*, Asteraceae) inferred from nrDNA ITS sequences. *Molec.*  
1130 *Phylogenet. Evol.* 25: 157–171. [http://dx.doi.org/10.1016/S1055-7903\(02\)00228-2](http://dx.doi.org/10.1016/S1055-7903(02)00228-2)
- 1131 **Galbany-Casals, M., Andrés-Sánchez, S., Garcia-Jacas, N., Susanna, A., Rico, E. & Martínez-**  
1132 **Ortega, M.M.** 2010. How many of Cassini anagrams should there be? Molecular systematics  
1133 and phylogenetic relationships in the *Filago* group (Asteraceae, Gnaphalieae), with special focus  
1134 on the genus *Filago*. *Taxon* 59: 1671–1689.
- 1135 **Galbany-Casals, M., Blanco-Moreno, J.M., Garcia-Jacas, N., Breitwieser, I. & Smissen, R.D.** 2011.  
1136 Genetic and morphological variation in the Mediterranean *Helichrysum italicum* (Asteraceae;  
1137 Gnaphalieae): do disjunct populations of subsp. *microphyllum* have a common origin? *Plant*  
1138 *Biol.* 13: 678–687. <http://dx.doi.org/10.1111/j.1438-8677.2010.00411.x>
- 1139 **Galbany-Casals, M., Carnicero-Campmany, P., Blanco-Moreno, J.M. & Smissen, R.D.** 2012.  
1140 Morphological and genetic evidence of contemporary intersectional hybridization in  
1141 Mediterranean *Helichrysum* (Asteraceae, Gnaphalieae). *Plant Biol.* 14: 789–800.  
1142 <http://dx.doi.org/10.1111/j.1438-8677.2012.00568.x>
- 1143 **Galbany-Casals, M., Garcia-Jacas, N., Sáez, L., Benedí, C. & Susanna, A.** 2009. Phylogeny,  
1144 biogeography, and character evolution in Mediterranean, Asiatic and Macaronesian *Helichrysum*  
1145 (Asteraceae, Gnaphalieae) inferred from nuclear phylogenetic analyses. *Int. J. Plant Sci.* 170:  
1146 365–380. <http://dx.doi.org/10.1086/596332>
- 1147 **Galbany-Casals, M., Sáez, L. & Benedí, C.** 2006a. A taxonomic revision of *Helichrysum* Mill. sect.  
1148 *Stoechadina* (DC.) Gren. & Godr. (Asteraceae, Gnaphalieae). *Canad. J. Bot.* 84: 1203–1232.  
1149 <http://dx.doi.org/10.1139/b06-082>
- 1150 **Galbany-Casals, M., Sáez, L. & Benedí, C.** 2006b. Conspectus of *Helichrysum* Mill. sect. *Stoechadina*  
1151 (DC.) Gren & Godr. (Asteraceae, Gnaphalieae). *Orsis* 21: 58–81.
- 1152 **Galbany-Casals, M., Sáez, L., Benedí, C. & Jarvis, C.E.** 2006c. Typification of names in *Gnaphalium*  
1153 *L.* and *Helichrysum* Mill. (Asteraceae), and some taxonomic notes. *Taxon* 55: 489–501.  
1154 <https://doi.org/10.2307/25065597>
- 1155 **Galbany-Casals, M., Unwin, M., Garcia-Jacas, N., Smissen R.D., Susanna, A. & Bayer R.J.** 2014.  
1156 Phylogenetic relationships in *Helichrysum* (Compositae: Gnaphalieae) and related genera:  
1157 Incongruence implications for generic delimitation. *Taxon* 63: 608–624.  
1158 <http://dx.doi.org/10.12705/633.8>
- 1159 **Giardina, G., Raimondo, F.M. & Spadaro, V.** 2007. A catalogue of the plants growing in Sicily.  
1160 *Bocconea* 20: 5–584.
- 1161 **Gil, L.** 1994. Biología reproductiva de la flora litoral de las Islas Baleares. I. Dunas y roquedos  
1162 marítimos. Unpublished PhD Thesis, University of the Balearic Islands, Palma de Mallorca.
- 1163 **Greuter, W.** (2006+): Compositae (pro parte majore). In: Greuter, W. & Raab-Straube, E. von (eds.):  
1164 Compositae. Euro+Med Plantbase - the information resource for Euro-Mediterranean plant  
1165 diversity. <http://ww2.bgbm.org/EuroPlusMed/> (accessed on Aug 2015)
- 1166 **Grimm, G.W. & Denk, T.** 2008. ITS evolution in *Platanus* (Platanaceae): homoeologues, pseudogenes  
1167 and ancient hybridization. *Ann. Bot.* 101: 403–419. <http://dx.doi.org/10.1093/aob/mcm305>
- 1168 **Gussone, G.** 1844. *Florae siculae synopsis exhibens plantas vasculares in Sicilia insulisque adjacentibus*  
1169 *huc usque detectas secundum systema linneanum depositas* 2. Napoli.
- 1170 **Guzmán, B. & Vargas, P.** 2009. Long distance colonisation by the Mediterranean *Cistus ladanifer*  
1171 (Cistaceae) despite the absence of special dispersal mechanisms. *J. Biogeogr.* 36: 954–968.  
1172 <http://dx.doi.org/10.1111/j.1365-2699.2008.02040.x>
- 1173 **Hilpold, A., Schönswetter, P., Susanna, A., Garcia-Jacas, N. & Vilatersana, R.** 2011. Evolution of the  
1174 central Mediterranean *Centaurea cineraria* group (Asteraceae): evidence for relatively recent,  
1175 allopatric diversification following transoceanic seed dispersal. *Taxon* 60: 528–538.
- 1176 **Hsü, K.J., Montardet, P., Bernoulli, D., Cita, M.B., Erickson, A., Garrison, R.E., Kidd, R., Mèlierés,**  
1177 **F., Müller, C. & Wright, R.** 1977. History of the Mediterranean salinity crisis. *Nature* 267: 399–  
1178 403. <http://dx.doi.org/10.1038/267399a0>

- 1179 **Huson, D.H. & Bryant, D.** 2006. Application of phylogenetic networks in evolutionary studies. *Molec.*  
1180 *Biol. Evol.* 23: 254–267. <http://dx.doi.org/10.1093/molbev/msj030>
- 1181 **Jackson, H.D., Steane, D.A., Potts, B.M. & Vaillancourt, R.E.** 1999. Chloroplast DNA evidence for  
1182 reticulate evolution in *Eucalyptus* (Myrtaceae). *Molec. Ecol.* 8: 739–751.  
1183 <http://dx.doi.org/10.1046/j.1365-294X.1999.00614.x>
- 1184 **Jolliffe, I.T.** 2002. *Principal Component Analysis*. 2nd ed. New York: Springer Series in Statistics.
- 1185 **Junikka, L., Uotila, P. & Lahti, T.** 2006. A phytogeographical comparison of the major Mediterranean  
1186 islands on the basis of Atlas Florae Europaeae. *Willdenowia* 36: 379–388.  
1187 <http://dx.doi.org/10.3372/wi.36.36134>
- 1188 **Koch, M.A., Karl, R., & German, D.A.** 2016. Underexplored biodiversity of Eastern Mediterranean  
1189 biota: systematics and evolutionary history of the genus *Aubrieta* (Brassicaceae). *Ann. Bot.* 119:  
1190 39–57. <http://dx.doi.org/10.1093/aob/mcw204>
- 1191 **Lavergne, S., Hampe, A. & Arroyo, J.** 2013. In and out of Africa: How did the Strait of Gibraltar affect  
1192 plant species migration and local diversification? *J. Biogeogr.* 40: 24–36.  
1193 <http://dx.doi.org/10.1111/j.1365-2699.2012.02769.x>
- 1194 **Lee, J.H., Lee, D.H. & Choi, B.H.,** 2013. Phylogeography and genetic diversity of East Asian *Neolitsea*  
1195 *sericea* (Lauraceae) based on variations in chloroplast DNA sequences. *J. Plant. Res.* 126: 193–  
1196 202. <http://dx.doi.org/10.1007/s10265-012-0519-1>
- 1197 **Linder, C.R., Goertzen, L.R., Heuvel, B.V., Francisco-Ortega, J. & Jansen, R.K.** 2000. The complete  
1198 external transcribed spacer of 18S-26S rDNA: Amplification and phylogenetic utility at low  
1199 taxonomic levels in Asteraceae and closely allied families. *Molec. Phylogenet. Evol.* 14: 285–  
1200 303. <http://dx.doi.org/10.1006/mpev.1999.0706>
- 1201 **Lo Presti, R.M. & Oberprieler, C.** 2011. The central Mediterranean as a phytodiversity hotchpotch:  
1202 phytogeographical patterns of the *Anthemis secundiramea* group (Compositae, Anthemideae)  
1203 across the Sicilian Channel. *J. Biogeogr.* 38: 1109–1124. <http://dx.doi.org/10.1111/j.1365-2699.2010.02464.x>
- 1204
- 1205 **Lojacono Pojero, M.** 1889–1908. *Flora Sicula*, vol. 5. Palermo: Tip. Vzi.
- 1206 **Lumaret, R., Mir, C., Michaud, H. & Raynal, V.** 2002. Phylogeographical variation of chloroplast  
1207 DNA in holm oak (*Quercus ilex* L.). *Molec. Ecol.* 11: 2327–2336.  
1208 <http://dx.doi.org/10.1046/j.1365-294X.2002.01611.x>
- 1209 **Manni, F., Guerard, E. & Heyer, E.** 2004. Geographic patterns of (genetic, morphologic, linguistic)  
1210 variation: how barriers can be detected by using Monmonier's algorithm. *Hum. Biol.* 76: 173–  
1211 190. <http://dx.doi.org/10.1353/hub.2004.0034>
- 1212 **Markos, S. & Baldwin, B.G.** 2001. Higher-level relationships and major lineages of *Lessingia*  
1213 (Compositae, Astereae) based on nuclear rDNA internal and external transcribed spacers (ITS  
1214 and ETS) sequences. *Syst. Bot.* 26: 168–183.
- 1215 **Mateo, G.** 2005. De Flora Valentina, VIII. *Fl. Montib.* 29: 92–95.
- 1216 **Mateo, G. & Crespo, M.** 2008. Novedades taxonómicas y nomenclaturales para la Flora Valenciana. *Fl.*  
1217 *Montib.* 40: 60–70.
- 1218 **Mateo, G., Crespo, M.B. & Laguna, E.** 2013. *Flora Valentina. Flora Vasculare de la Comunidad*  
1219 *Valenciana*, vol. 2. Valencia: Fundación de la Comunidad Valenciana para el Medio Ambiente.
- 1220 **Moris, G.G.** 1840–1843. *Flora Sardoia*, vol. 2. Taurini: Regio Typographeo.
- 1221 **Müller, K.** 2006. Incorporating information from length-mutational events into phylogenetic analysis.  
1222 *Molec. Phylogenet. Evol.* 38: 667–676. <http://dx.doi.org/10.1016/j.ympev.2005.07.011>
- 1223 **Myers, N., Mittermeier, R.A., Mittermeier, C.G., Fonseca, G.A.B. & Kent, J.** 2000. Biodiversity  
1224 hotspots for conservation priorities. *Nature* 403: 853–858. <http://dx.doi.org/10.1038/35002501>
- 1225 **Nei, M.** 1972. Genetic distances between populations. *Am. Nat.* 106: 283–291.  
1226 <https://doi.org/10.1086/282771>
- 1227 **Nie, Z. L., Funk, V. A., Meng, Y., Deng, T., Sun, H. & Wen, J.** 2016. Recent assembly of the global  
1228 herbaceous flora: evidence from the paper daisies (Asteraceae: Gnaphalieae). *New Phytol.* 209:  
1229 1795–1806. <http://dx.doi.org/10.1111/nph.13740>
- 1230 **Nieto-Feliner, G.** 2014. Patterns and processes in plant phylogeography in the Mediterranean Basin. A  
1231 review. *Perspect. Plant Ecol. Evol. Syst.* 16: 265–278.  
1232 <http://dx.doi.org/10.1016/j.ppees.2014.07.002>
- 1233 **Nyman, C.F.** 1879. *Conspectus florae Europaeae seu. Örebro; Officinae Bohlinianae.*
- 1234 **Ortiz, M.Á., Tremetsberger, K., Talavera, S., Stuessy, T. & García-Castro, L.** 2007. Population  
1235 structure of *Hypochaeris salzmanniana* DC. (Asteraceae), an endemic species to the Atlantic  
1236 coast on both sides of the Strait of Gibraltar, in relation to Quaternary sea level changes. *Molec.*  
1237 *Ecol.* 16: 541–552. <http://dx.doi.org/10.1111/j.1365-294X.2006.03157.x>

- 1238 **Peakall, R. & Smouse, P.E.** 2012. GenAlEx 6.5: genetic analysis in Excel. Population genetic software  
1239 for teaching and research - an update. *Bioinformatics* 28: 2537–2539.  
1240 <http://dx.doi.org/10.1093/bioinformatics/bts460>
- 1241 **Petit, R.J., Aguinalalde, I., de Beaulieu, J.-L., Bittkau, Ch., Brewer, S., Cheddadi, R., Ennos, R.,**  
1242 **Fineschi, S., Grivet, D., Lascoux, M., Mohanty, A., Müller-Starck, G., Demesure-Musch, B.,**  
1243 **Palmé, A., Martín J.P., Rendell, S., Vendramin, G.G.** 2003. Glacial refugia: Hotspots but not  
1244 melting pots of genetic diversity. *Science* 300: 1563–1565.  
1245 <http://dx.doi.org/10.1126/science.1083264>
- 1246 **Pignatti, S.** 1980. Note critiche sulla Flora d'Italia. VI. Ultimi appunti miscellanei. *Giorn. Bot. Ital.* 113:  
1247 359–368. <https://doi.org/10.1080/11263507909426411>
- 1248 **Pignatti, S.** 1982. *Flora d'Italia*, vol. 3. Bologna: Edagricole.
- 1249 **Posada, D.** 2008. jModelTest: Phylogenetic model averaging. *Molec. Biol. Evol.* 25: 1253–1256.  
1250 <http://dx.doi.org/10.1093/molbev/msn083>
- 1251 **Presl, K.B.** 1826. *Flora Sicula, exhibens plantas vasculosas in Sicilia aut sponte crescentes aut*  
1252 *frequentissime cultas, secundum systema naturale digestas*, vol. 1. Pragae: Sumptibus A.  
1253 Borrosch.
- 1254 **Rambaut, A.** 2009. FigTree v.3.1. <http://tree.bio.ed.ac.uk/software/figtree/> (accessed on 2014-6).
- 1255 **Rambaut, A., Suchard, M.A., Xie, D. & Drummond, A.J.** 2013. Tracer v1.6.  
1256 <http://beast.bio.ed.ac.uk/software/tracer/> (accessed on 2014-6).
- 1257 **Rodríguez-Sánchez, F., Pérez-Barrales, R., Ojeda, F., Vargas, P. & Arroyo, J.** 2008. The Strait of  
1258 Gibraltar as a melting pot for plant biodiversity. *Quat. Sci. Rev.* 27: 2100–2117.  
1259 <http://dx.doi.org/10.1016/j.quascirev.2008.08.006>
- 1260 **Ronikier, M., Schneeweiss, G.M., & Schönswetter, P.** 2012. The extreme disjunction between Beringia  
1261 and Europe in *Ranunculus glacialis* s.l. (Ranunculaceae) does not coincide with the deepest  
1262 genetic split – a story of the importance of temperate mountain ranges in arctic-alpine  
1263 phylogeography. *Molec. Ecol.* 21: 5561–5578. <http://dx.doi.org/10.1111/mec.12030>
- 1264 **Ronquist, F. & Huelsenbeck, J.P.** 2003. MRBAYES 3: Bayesian phylogenetic inference under mixed  
1265 models. *Bioinformatics* 19: 1572–1574. <http://dx.doi.org/10.1093/bioinformatics/btg180>
- 1266 **Rosenbaum, G., Lister, G.S. & Duboz, C.** 2002. Reconstruction of the tectonic evolution of the western  
1267 Mediterranean since the Oligocene. *J. Virtual Explor.* 8: 107–130.  
1268 <http://dx.doi.org/10.3809/jvirtex.2002.00053>
- 1269 **Rouy, G.** 1888. Excursions botaniques en Espagne. *Bull. Soc. Bot. France* 35: 115–124.  
1270 <https://doi.org/10.1080/00378941.1888.10830325>
- 1271 **Rubio de Casas, R., Besnard, G., Schönswetter, P., Balaguer, L. & Vargas, P.** 2006. Extensive gene  
1272 flow blurs phylogeographic but not phylogenetic signal in *Olea europaea* L. *Theor. Appl. Genet.*  
1273 113: 575–583. <http://dx.doi.org/10.1007/s00122-006-0306-2>
- 1274 **Schlick-Steiner, B.C., Steiner, F.M., Seifert, B., Stauffer, C., Christian, E., & Crozier, R.H.** 2010.  
1275 Integrative taxonomy: a multisource approach to exploring biodiversity. *Annu. Rev. Entomol.* 55:  
1276 421–438. <http://dx.doi.org/10.1146/annurev-ento-112408-085432>
- 1277 **Scialabba, A., Agrimonti, C., Abbate, G.M. & Marmiroli, N.** 2008. Assessment of genetic variation in  
1278 Sicilian *Helichrysum* (Asteraceae) and implications to germplasm conservation. *Plant Biosys.*  
1279 142: 287–297. <http://dx.doi.org/10.1080/11263500802150530>
- 1280 **Sciberras, J. & Sciberras, A.** 2009. Notes on the distribution of *Helichrysum melitense*, *Hyoseris*  
1281 *frutescens* and *Matthiola incana* subsp. *melitensis* in the Maltese Islands. *The Central*  
1282 *Mediterranean Naturalist* 5: 28–34.
- 1283 **Shaw, J., Lickey, E.B., Schilling, E.E. & Small, R.L.** 2007. Comparison of whole chloroplast genome  
1284 sequences to choose noncoding regions for phylogenetic studies in angiosperms: The tortoise and  
1285 the hare III. *Am. J. Bot.* 94: 275–288. <http://dx.doi.org/10.3732/ajb.94.3.275>
- 1286 **Smitsen, R.D., Breitwieser, I. & Wardm J.M.** 2004. Phylogenetic implications of trans-specific  
1287 chloroplast DNA sequence polymorphism in New Zealand Gnaphalieae (Asteraceae). *Plant Syst.*  
1288 *Evol.* 249: 37–53. <http://dx.doi.org/10.1007/s00606-004-0209-0>
- 1289 **Smitsen, R. D., Breitwieser, I. & Ward, J. M.** 2007. Genetic characterization of hybridization between  
1290 the New Zealand everlastings *Helichrysum lanceolatum* and *Anaphalioides bellidioides*  
1291 (Asteraceae: Gnaphalieae). *Bot. J. Linn. Soc.* 154: 89–98. [http://dx.doi.org/10.1111/j.1095-](http://dx.doi.org/10.1111/j.1095-8339.2007.00632.x)  
1292 [8339.2007.00632.x](http://dx.doi.org/10.1111/j.1095-8339.2007.00632.x)
- 1293 **Smitsen, R. D., Galbany-Casals, M. & Breitwieser, I.** 2011. Ancient allopolyploidy in the everlasting  
1294 daisies (Asteraceae: Gnaphalieae): complex relationships among extant clades. *Taxon* 60: 649–  
1295 662.
- 1296 **Stephens, M., Smith, N.J. & Donnelly, P.** 2001. A new statistical method for haplotype reconstruction  
1297 from population data. *Am. J. Hum. Genet.* 68: 978–989. <http://dx.doi.org/10.1086/319501>



- 1298 **Stöck, M., Sicilia, A., Belfiore, N.M., Buckley, D., Lo Brutto, S., Lo Valvo, M. & Arculeo, M.** 2008.  
1299 Post Messinian evolutionary relationships across the Sicilian channel: mitochondrial and nuclear  
1300 markers link a new green toad from Sicily to African relatives. *B.M.C. Evol. Biol.* 8: 56.  
1301 <http://dx.doi.org/10.1186/1471-2148-8-56>
- 1302 **Swofford, D.L.** 2002. PAUP\*: Phylogenetic analysis using parsimony (\*and other methods), version 4.0  
1303 Beta. Sunderland: Sinauer.
- 1304 **Tamura, K., Stecher, G., Peterson, D., Filipiński, A. & Kumar, S.** 2013. MEGA6: Molecular  
1305 evolutionary genetics analysis version 6.0. *Molec. Biol. Evol.* 30: 2725–2729.  
1306 <http://dx.doi.org/10.1093/molbev/mst197>
- 1307 **Tel-Zur, N., Abbo, S., Myslabodski, D. & Mizrahi, Y.** 1999. Modified CTAB procedure for DNA  
1308 isolation from epiphytic cacti of genera *Hylocereus* and *Selenicereus* (Cactaceae). *Plant Molec.*  
1309 *Biol. Rep.* 17: 249–254. <http://dx.doi.org/10.1023/A:1007656315275>
- 1310 **Templeton, A.R., Crandall, K.A. & Sing, C.F.** 1992. A cladistic analysis of phenotypic associations with  
1311 haplotypes inferred from restriction endonuclease mapping and DNA sequence data. III.  
1312 Cladogram estimation. *Genetics* 123: 585–595.
- 1313 **Terrab, A., Schönewetter, P., Talavera, S., Vela, E. & Stuessy, T.F.** 2008. Range-wide phylogeography  
1314 of *Juniperus thurifera* L., a presumptive keystone species of western Mediterranean vegetation  
1315 during cold stages of the Pleistocene. *Molec. Phylogenet. Evol.* 48: 94–102.  
1316 <http://dx.doi.org/10.1016/j.ympev.2008.03.018>
- 1317 **Thompson, J.D.** 2005. *Plant evolution in the Mediterranean*. Oxford: Oxford University Press.  
1318 <https://doi.org/10.1093/acprof:oso/9780198515340.001.0001>
- 1319 **Troia, A., Raimondo, F.M. & Geraci, A.** 2012. Does genetic population structure of *Ambrosina bassii* L.  
1320 (Araceae, Ambrosineae) attest a post-Messinian land-bridge between Sicily and Africa? *Flora*  
1321 207: 646–653. <http://dx.doi.org/10.1016/j.flora.2012.06.017>
- 1322 **Valdés, B., Talavera, S. & Fernández-Galiano, E. (eds.).** 1987. *Flora Vascular de Andalucía*  
1323 *Occidental*, vol. 3. Barcelona: Ketres editora.
- 1324 **Wallmann, P.C., Mahood, G.A. & Pollard, D.D.** 1988. Mechanical models for correlation of ring-  
1325 fracture eruptions at Pantelleria, Strait of Sicily, with glacial sea-level drawdown. *Bull. Volc.* 50:  
1326 327–339. <https://doi.org/10.1007/bf01073589>
- 1327 **Wendel, J.F. & Doyle, J.J.** 1998. Phylogenetic incongruence: Window into genome history and  
1328 molecular evolution. Pp. 256–296 in: Soltis, D.E., Soltis, P.S. & Doyle, J.J. (eds.), *Molecular*  
1329 *systematics of plants II. DNA sequencing*. Boston: Kluwer Academic Publishers.  
1330 [http://dx.doi.org/10.1007/978-1-4615-5419-6\\_10](http://dx.doi.org/10.1007/978-1-4615-5419-6_10)
- 1331 **Woodward, J.C.** 2009. *The physical geography of the Mediterranean*. Oxford: Oxford University Press.
- 1332 **Xiberras, J.** 2013. *Population studies on Helichrysum melitense*. Malta: Department of Biology,  
1333 University of Malta.
- 1334 **Yeates, D.K., Seago, A., Nelson, L., Cameron, S.L., Joseph, L. & Trueman, J.W.** 2011. Integrative  
1335 taxonomy, or iterative taxonomy? *Syst. Entomol.* 36: 209–217. <http://dx.doi.org/10.1111/j.1365-3113.2010.00558.x>
- 1337 **Yokoyama, Y., Lambeck, K., De Deckker, P., Johnston, P. & Fifield, L.K.** 2000. Timing of the Last  
1338 Glacial Maximum from observed sea-level minima. *Nature* 406: 713–716.  
1339 <http://dx.doi.org/10.1038/35021035>
- 1340 **Zozomová-Lihová, J., Marhold, K. & Španiel, S.** 2014. Taxonomy and evolutionary history of *Alyssum*  
1341 *montanum* (Brassicaceae) and related taxa in southwestern Europe and Morocco: Diversification  
1342 driven by polyploidy, geographic and ecological isolation. *Taxon* 63: 562–591.  
1343 <http://dx.doi.org/10.12705/633.18>
- 1344  
1345  
1346  
1347  
1348  
1349  
1350  
1351  
1352  
1353  
1354  
1355  
1356  
1357

1358  
1359  
1360  
1361  
1362  
1363  
1364  
1365  
1366  
1367  
1368  
1369  
1370  
1371  
1372

**Table 1.** Morphological variables used in morphometric analyses. Type of characters are: qualitative (QL), quantitative (QN) and semiquantitative (SQN).

Morphological characters	Type of character
Vegetative characters	
1. Presence (1) / absence (0) of succulent leaves <sup>1</sup>	QL
2. Basal and median cauline leaf length (mm)	QN
3. Basal and median cauline leaf width (mm)	QN
4. Basal and median cauline leaf length / width	QN
5. Basal and median leaf margin (flat or revolute) (0–4) <sup>2</sup>	SQN
6. Eglanular indumentum of adaxial leaf side (0–4) <sup>3</sup>	SQN
7. Glandular indumentum of abaxial leaf side (0–4) <sup>3</sup>	SQN
Floral characters	
8. Synflorescence length (mm)	QN
9. Synflorescence width (mm)	QN
10. Synflorescence length / synflorescence width	QN
11. Number of capitula per synflorescence	QN
12. Synflorescence density <sup>4,5</sup>	QN
13. Capitulum length (mm)	QN
14. Capitulum width (mm)	QN
15. Capitulum length / capitulum width	QN
16. Number of pistillate florets per capitulum	QN
17. Number of hermaphroditic florets per capitulum	QN
18. Total number of florets per capitulum	QN
19. Number of pistillate florets per capitulum / total number of florets per capitulum	QN
20. Outermost involucre bract length (mm)	QN
21. Outermost involucre bract width (mm)	QN
22. Outermost involucre bract length / outermost involucre bract width	QN
23. Outermost involucre bract texture (0–1) <sup>6</sup>	SQN
24. Eglanular indumentum of outermost involucre bract (0–4) <sup>3</sup>	SQN
25. Innermost involucre bract length (mm)	QN
26. Innermost involucre bract width (mm)	QN
27. Innermost involucre bract length / innermost involucre bract width	QN
28. Eglanular indumentum of innermost involucre bract (0–4) <sup>3,7</sup>	SQN
29. Glandular indumentum of innermost involucre bract (0–4) <sup>3</sup>	SQN
30. Average of innermost involucre bract length / outermost involucre bract length	QN
31. Number of involucre bracts per capitulum	QN

1373  
1374  
1375  
1376  
1377  
1378  
1379  
1380  
1381  
1382  
1383  
1384  
1385

<sup>1</sup> Only used in PCA3.

<sup>2</sup> 0: all leaves flat; 1: most leaves flat, some revolute; 2: flat and revolute leaves in the same proportion; 3: most leaves revolute, some flat; 4: all leaves revolute.

<sup>3</sup> 0: 0–5% coverage; 1: 6–25% coverage; 2: 26–50% coverage; 3: 51–75% coverage; 4: 76–100% coverage.

<sup>4</sup> Number of capitula per synflorescence / (synflorescence length × synflorescence width).

<sup>5</sup> Only used in PCA3 and CDA because data were not available for all specimens.

<sup>6</sup> 0: bract totally papery; 0.5: bract herbaceous in its basal half and papery in its distal half; 1: bract totally herbaceous.

<sup>7</sup> Only two states in PCA3 and was coded as qualitative in that analysis.

1386  
1387  
1388  
1389  
1390  
1391  
1392  
1393  
1394  
1395  
1396  
1397  
1398  
1399  
1400  
1401  
1402  
1403  
1404

**Table 2.** Analyses of molecular variance (AMOVA) based on the *rpl32-trnL* spacer and ETS sequence data for the *Helichrysum pendulum* complex

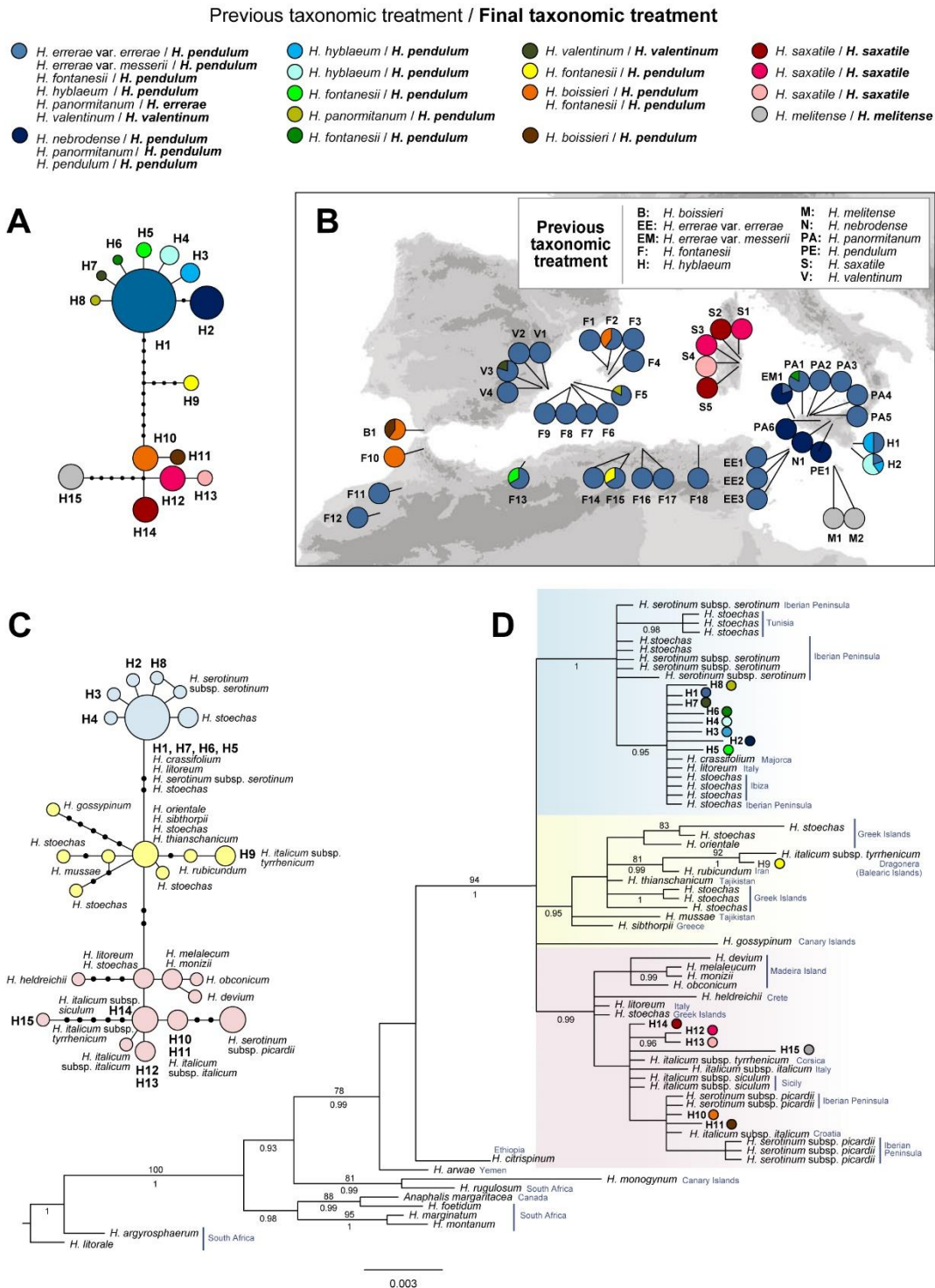
	Sources of variation	<i>rpl32-trnL</i> spacer				ETS			
		df	Sum of squares	% variation	Fixation indices	df	Sum of squares	% variation	Fixation indices
<b>Assuming no regional differentiation</b>	Between populations	43	1088.02	87.30	$\Phi_{ST} = 0.87^*$	41	935.09	83.89	$\Phi_{ST} = 0.84^*$
	Within populations	172	125.47	12.70		158	140.40	16.11	
<b>Assuming regional differentiation</b>	Between western-central groups <sup>1</sup>	1	6.41	4.73	$F_{SC} = 0.87^*$	1	393.04	54.63	$F_{SC} = 0.75^*$
	Between populations within groups <sup>1</sup>	42	1031.61	82.87	$\Phi_{ST} = 0.88^*$	40	542.04	34.08	$\Phi_{ST} = 0.89^*$
	Within populations	172	125.47	12.41	$F_{CT} = 0.05$	158	140.40	11.29	$F_{CT} = 0.55^*$
	Between geographical groups <sup>2</sup>	13	866.47	66.91	$F_{SC} = 0.64^*$	13	705.44	58.16	$F_{SC} = 0.63^*$
	Between populations within groups <sup>2</sup>	30	221.55	21.27	$\Phi_{ST} = 0.88^*$	28	229.65	26.53	$\Phi_{ST} = 0.85^*$
	Within populations	172	125.47	11.82	$F_{CT} = 0.67^*$	158	140.40	15.31	$F_{CT} = 0.58^*$

1405  
1406  
1407  
1408  
1409  
1410  
1411  
1412  
1413

<sup>1</sup> Western-central groups: western Mediterranean group includes Majorca, Ibiza, Imperialet, Vedranell, Es Vedrà, Alicante, Gibraltar, Morocco and Algeria; central Mediterranean group includes Sardinia, Sicily, Marettimo, Pantelleria and Malta.

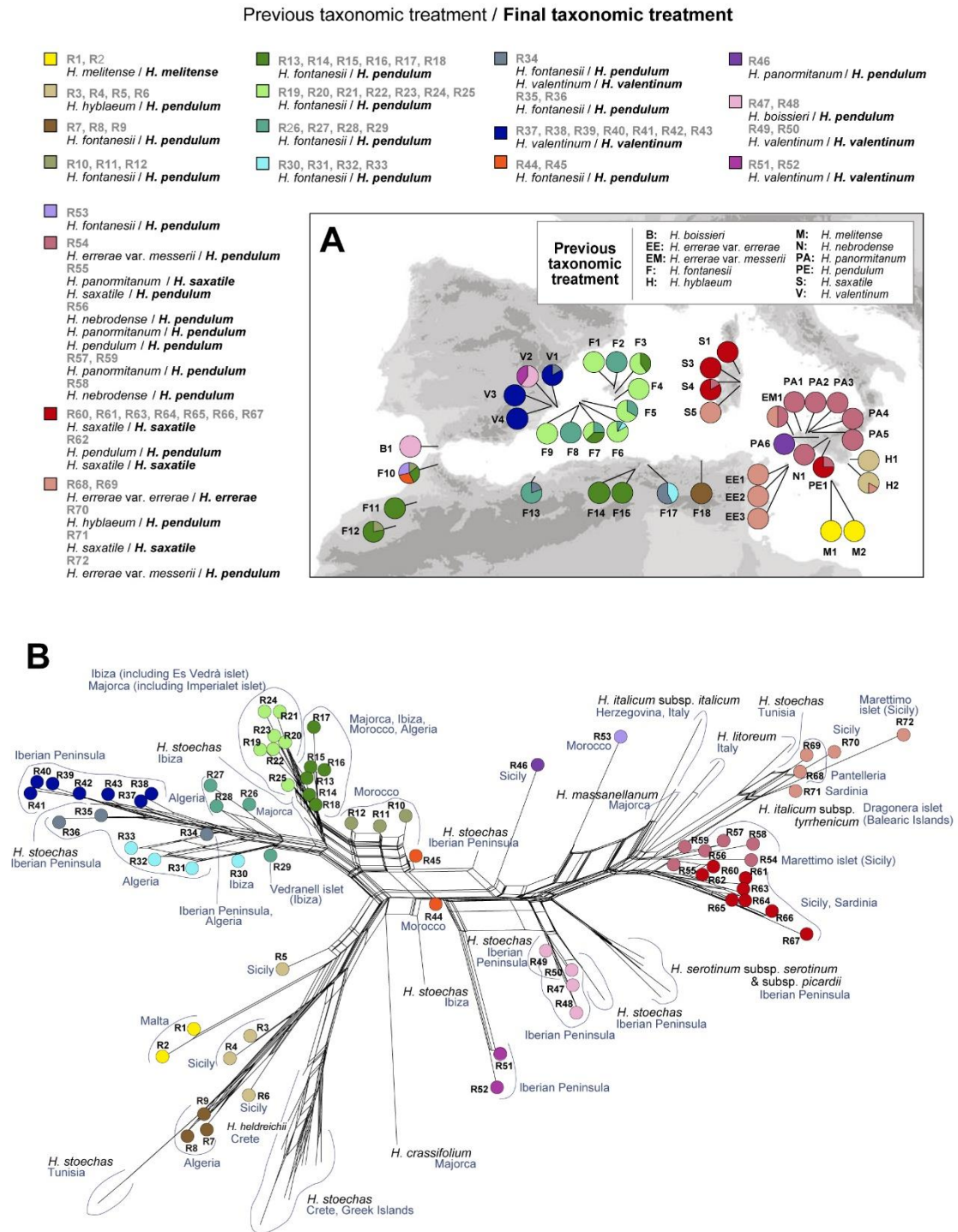
<sup>2</sup> Geographical groups: Majorca, Imperialet, Ibiza, Vedranell, Es Vedrà, Alicante, Gibraltar, Morocco, Algeria, Sardinia, Sicily, Marettimo, Pantelleria and Malta.

\*  $p < 0.001$  (significant after 1023 permutations)



1414  
1415  
1416  
1417  
1418  
1419  
1420  
1421  
1422  
1423  
1424  
1425  
1426

**Fig. 1.** **A**, Parsimony network relationships of the 15 different haplotypes found in the 216 individuals of the *Helichrysum pendulum* complex. The size of circles is proportional to the frequency of each haplotype in the total sample. Small black circles represent intermediate haplotypes that were not detected. Lines between circles represent one mutational step. **B**, Geographical distribution of the 15 different haplotypes obtained. For population abbreviation codes and additional information see [Electr. Suppl.: Table S1](#). **C**, Parsimony network relationships of the 15 haplotypes detected in the *H. pendulum* complex and the other species of the Mediterranean-Macaronesian-Asiatic clade. **D**, Phylogram obtained from Bayesian analysis of the 15 haplotypes detected and the rest of the species included in the study (dataset 3, see text for details). Bootstrap values from the maximum parsimony analysis are shown above and Bayesian posterior probabilities are shown below branches.



1427  
1428  
1429  
1430  
1431  
1432  
1433  
1434  
1435

**Fig. 2. A**, Geographic distribution of the 72 different ribotypes found in 159 individuals from 42 populations of the *H. pendulum* complex. To simplify the representation of the ribotypes, they have been reduced to 18 colour groups (see text for details). **B**, Neighbour-Net graph derived from the 72 ribotypes detected in the *H. pendulum* complex and 38 ribotypes detected in other taxa of sect. *Stoechadina* (see text for details) Geographical origin in blue. For population abbreviation codes and the specimens containing each ribotype see [Electr. Suppl.: Table S1](#).

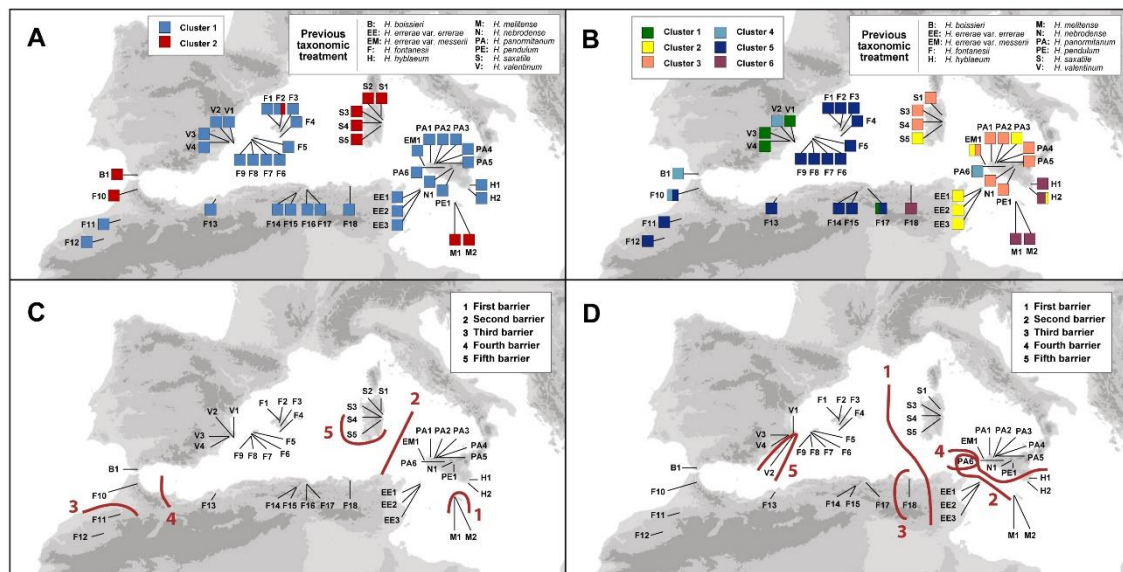


**Fig. 3. A-B**, BAPS analysis of the *H. pendulum* complex. **A**, using cpDNA sequences ( $K = 2$ ). **B**, using nrDNA sequences ( $K = 6$ ). **C-D**, The first five barriers detected in the *H. pendulum* complex using Monmonier's maximum difference algorithm with Nei's genetic distances. **C**, from the cpDNA sequences. **D**, from the nrDNA.

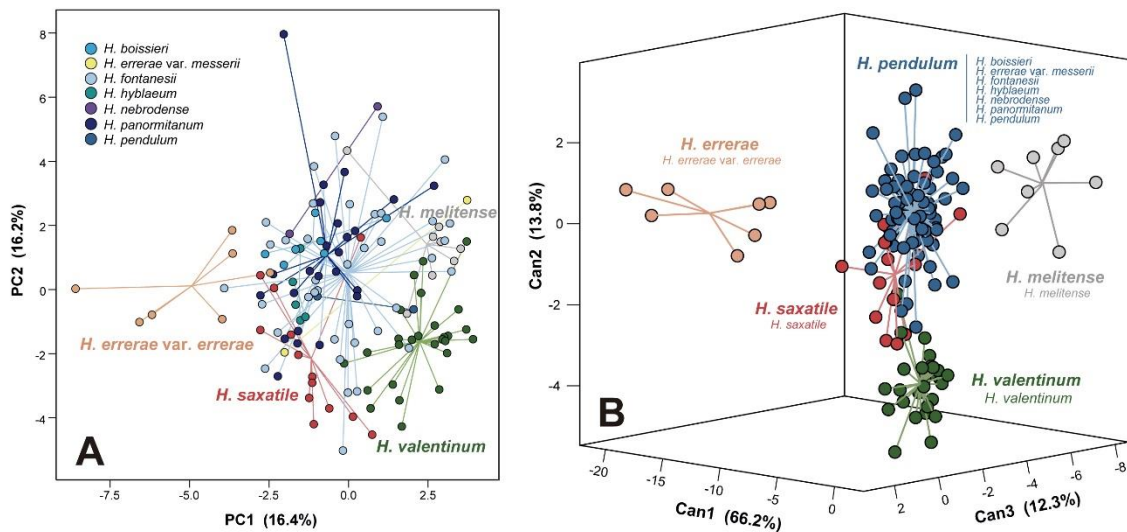
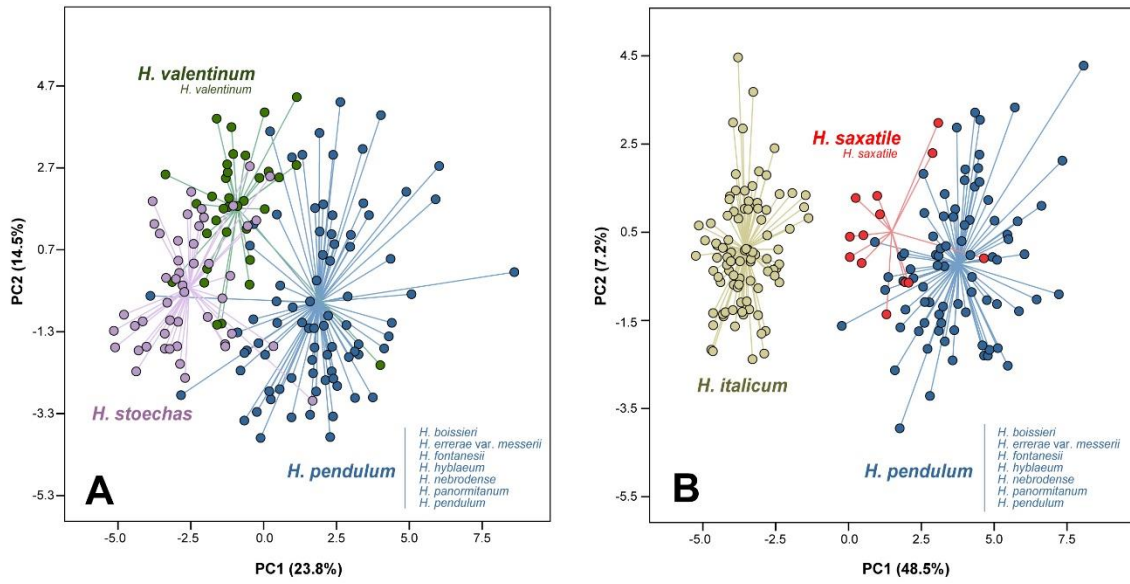
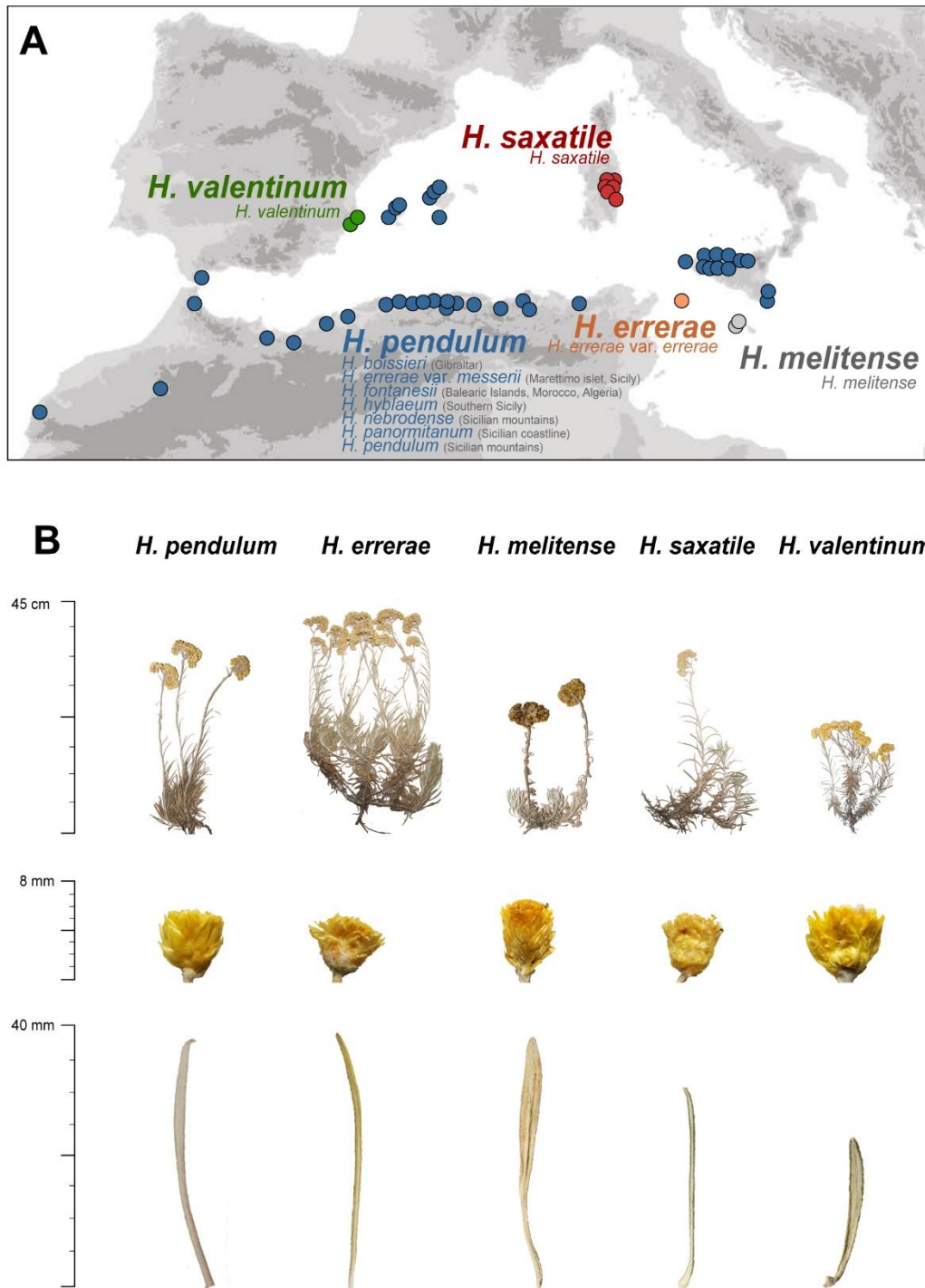


**Fig. 4. A**, Scatterplot of the first two axes from the Principal Component Analysis (PCA3) based on 31 morphological characters studied in 136 individuals: 7 individuals of *H. boissieri*, 7 of *H. errerae* var. *errerae*, 2 of *H. errerae* var. *messenii*, 38 of *H. fontanesii*, 5 of *H. hyblaenum*, 8 of *H. melitense*, 2 of *H. nebrodenses*, 24 of *H. panormitanum*, 2 of *H. pendulum*, 13 of *H. saxatile* and 28 of *H. valentinum*. Taxa are labelled following previous taxonomic treatments (see text for details). **B**, Scatterplot of the Canonical Discriminant Analysis (CDA) based on 29 morphometric variables for the 136 individuals classified in five predefined groups, the final taxonomic treatment, considering molecular and morphological data: *H. errerae*, *H. melitense*, *H. pendulum*, *H. saxatile* and *H. valentinum*. Previous taxonomic treatment and final taxonomic treatment (in bold) are given.



1457  
1458  
1459  
1460  
1461  
1462  
1463  
1464  
1465  
1466  
1467

**Fig. 5. A,** Scatterplot of the first two axes from the Principal Component Analysis (PCA4) based on 29 morphological characters studied for a total of 156 individuals: 28 individuals of *H. valentinum*, 80 of *H. pendulum* and 48 of *H. stoechas*. Previous taxonomic treatment and final taxonomic treatment (in bold) are indicated. **B,** Scatterplot of the first two axes from the Principal Component Analysis (PCA5) based on 29 morphological characters studied for a total of 183 individuals: 13 individuals of *H. saxatile*, 80 of *H. pendulum* and 90 of *H. italicum*. Previous taxonomic treatment and final taxonomic treatment (in bold) are indicated.



1468  
1469  
1470  
1471  
1472  
1473

**Fig. 6. A**, Distribution area of the species of the *H. pendulum* complex recognised in this study. Previous taxonomic treatment and final taxonomic treatment (in bold) are indicated. **B**, Details of general appearance, capitula and leaves of each taxon finally recognized.